Article:
Abe, K., Afif, M.T., Ahl Laamara, R. et al. (2026) Sensitivity of the Hyper-Kamiokande experiment to neutrino oscillation parameters using accelerator neutrinos. The European Physical Journal C, 86 (2). 170. ISSN: 1434-6044

https://doi.org/10.1140/epjc/s10052-025-14938-9

Eur. Phys. J. C (2026) 86:170
https://doi.org/10.1140/epjc/s10052-025-14938-9

THE EUROPEAN PHYSICAL JOURNAL C

Regular Article - Experimental Physics

Sensitivity of the Hyper-Kamiokande experiment to neutrino oscillation parameters using accelerator neutrinos

Hyper-Kamiokande Collaboration[a]

K. Abe[1], M. T. Afif[2], R. Ahl Laamara[3], H. Aihara[4], A. Ajmi[5], R. Akutsu[6,b], H. Alarakia-Charles[7], I. Alekseev[116], Y. Alj Hakim[8], S. Alonso Monsalve[9], E. Amato[10], F. Ameli[11], L. Anthony[12], A. Araya[13], A. Arguello Quiroga[14], S. Arimoto[15], Y. Asaoka[1], Y. Ashida[16], V. Aushev[17], F. Ballester Merelo[18], M. Barbi[19], G. Barr[20], M. Batkiewicz-Kwasniak[21], A. Beauchêne[22], D. Benchekroun[23], V. Berardi[10,24], E. Bernardini[25,26], L. Berns[16], S. Bhadra[27], N. Bhuiyan[28], J. Bian[29], D. Bianco[30,h], A. Blanchet[31], A. Blondel[31], P. M. M. Boistier[32], S. Bolognesi[32], L. Bonavera[33], José L. Bonilla[34], S. Bordoni[35], D. Bose[36], S. Boyd[37], C. Bozza[38,39], A. Bravar[35], C. Bronner[40], A. Bubak[41], A. Buchowicz[42], M. Buizza Avanzini[22], G. Burton[28,43], F. S. Cafagna[10], N. F. Calabria[10,24], J. M. Calvo Mozota[44], S. Cao[45], D. Carabadjac[22,c], S. Cartwright[8], M. P. Casado[46,d], M. G. Catanesi[10], C. Cavanagh[9], S. Cebrián[47], E. M. Chakir[48], S. Chakrabarty[49], J. H. Choi[50], A. Choquet[2], S. Choubey[51], E. A. Chucuan Martinez[52], L. Chytka[53], M. Cicerchia[114], L. Cid Barrio[44], M. Cieślar[54,a], J. Coleman[55], G. Collazuol[25,26], L. Cook[56], F. Cormier[56], D. Costas-Rodríguez[57], A. Craplet[12], S. Cuen-Rochin[52], C. Dalmazzone[31], M. Danilov[117], M. Daoud[48], T. Daret[32], F. J. De Cos[33], E. de la Fuente[58,59], A. De Lorenzis[46,e], G. De Rosa[30,60], T. Dealtry[7], M. Della Valle[30], C. Densham[43], A. Dergacheva[118], M. M. Devi[61], F. Di Lodovico[28], A. Di Nitto[30,60], A. Di Nola[30,60], G. Díaz López[31], T. C. Dieminger[9], D. Divecha[19], M. Dobrzynska[62], T. Dohnal[63], T. Doyle[20], E. Drakopoulou[64], O. Drapier[22], C. Duarte Galvan[52], J. Dumarchez[31], K. Dygnarowicz[42], S. Earle[65], A. Eguchi[4], A. El Abassi[48], M. El Baz[35], A. El Kaftaoui[48], J. Ellis[28], R. Elmansali[66], S. Emery[32], R. Er-Rabit[48], A. Ershova[22], A. Esmaili[14], R. Esteve Bosch[18], G. Eurin[32], C. E. Falcón Anaya[52], L. E. Falcon Morales[67], J. Fannon[8], S. Fedotov[119], M. Feltre[25], J. Feng[15], D. Ferlewicz[31], P. Fernández-Menéndez[57], E. Fernández-Martinez[68], P. Ferrario[69], B. Ferrazzi[19], A. Finch[7], C. Finley[70], G. A. Fiorentini Aguirre[66], M. Fitton[43], M. Franks[9], M. Friend[6,b,f], Y. Fujii[6,b], Y. Fukuda[71], L. Fusco[38,39], R. Gaior[31], G. Galiński[42], R. Gamboa Goñi[67], J. Gao[28], F. Garcia Riesgo[33], C. Garde[72], R. Gaur[56], L. Gialanella[30,73], C. Giganti[31], V. Gligorov[31], O. Gogota[17], M. Gola[56], A. Goldsack[28], J. J. Gomez-Cadenas[69], M. Gonin[1,2], J. González-Nuevo[33], A. Gorin[1], R. Gornea[66], S. Goto[4], M. Gouighri[48], J. Gracia Rodriguez[33], K. Graham[66], F. Gramegna[114], M. Grassi[25,26], H. Griguer[74], M. Guigue[31], D. Hadley[37], A. Hambardzumyan[75], M. Harada[1], R. J. Harris[7,43], M. Hartz[56], E. Harvey-Fishenden[43], S. Hassani[32], N. C. Hastings[6,b], S. Hayashida[28], Y. Hayato[1], K. Hayrapetyan[28], I. Heitkamp[16], B. Hernandez-Molinero[44], J. A. Hernando Morata[57], V. Herrero Bosch[18], Y. Hino[6,b], K. Hiraide[1], J. Holeczek[41], A. Holin[43], S. Horiuchi[76], K. Hoshina[13,77], K. Hosokawa[115], A. Hoummada[23], F. Hrub y[53], H. Hua[65], K. Hultqvist[70], F. Iacob[25,26], A. K. Ichikawa[16], W. Idrissi Ibnsalih[30,73], K. Ieki[1], M. Ikeda[1], A. S. Inácio[20], A. Ioannisian[75], T. Ishida[6,b], K. Ishidoshiro[115], H. Ishino[78], M. Ishitsuka[79], H. Israel[8], H. Ito[80], Y. Itow[81,g], A. Izmaylov[120], S. Izumiyama[82], B. Jamieson[5], J. Jang[83], S. Jenkins[55], C. Jesús-Valls[84], H. S. Jo[85], T. P. Jones[7], P. Jonsson[12], K. K. Joo[86], S. Joshi[32], T. Kajita[87], H. Kakuno[88], L. Kalousis[64], J. Kameda[1], Y. Kano[13], D. Karlen[56,89], Y. Kataoka[1], A. Kato[13], T. Katori[28], N. Kazarian[75], M. Khabibullin[121], A. Khotjantsev[122], T. Kikawa[15], J. Y. Kim[86], S. King[28], J. Kisiel[41], J. Klimaszewski[62], L. Kneale[8], M. Kobayashi[76], T. Kobayashi[6,b,f], S. Kodama[4], L. Koerich[19], N. Kolev[19], H. Komaba[16], A. Konaka[56], L. Kormos[7], U. Kose[9], Y. Koshio[78], T. Kosinski[62], K. Kouzakov[123], K. Kowalik[62], R. Kralik[28], L. Kravchuk[1], A. Kryukov[124], Y. Kudenko[125], A. Kulkarni[72], T. Kumita[88], R. Kurjata[42], T. Kutter[90], M. Kuze[82], J. Kvita[53], K. Kwak[91], E. Kwon[92], L. Labarga[68], K. Lachner[9], J. Lagoda[62], G. Lamanna[93,94], M. Lamers James[37], A. Langella[30,60], J. Laporte[32], N. Latham[28], M. Laveder[25,26], L. Lavitola[30,60], M. Lawe[7], E. Le Blévec[2,22], J. Lee[85], R. Leitner[63], S. Levorato[25], S. Lewis[28],

Published online: 23 February 2026

B. Li[9], Q. Li[8], X. Li[56], I. Lim[86], U. Limbu[55], T. Lindner[56], R. P. Litchfield[95], Y. Liu[76], K. Long[12], A. Longhin[25,26], F. López-Gejo[69], A. Lopez Moreno[28], P. Lorens[42], P. Lu[56], X. Lu[20], L. Ludovici[11], T. Lux[46], Y. Maekawa[76], L. Magaletti[10,24], J. Mahesh[6,f], P. Maimí[96], Y. Makida[6,b], M. Malek[8], M. Malinský[63], M. Mandal[62], Y. Mandokoro[79], M. Mansoor[5], T. Marchi[114], C. Mariani[97], A. Marinelli[30], C. Markou[64], F. Maroufkhani[89], K. Martens[84], L. Marti[1,84], J. Martin[98], L. Martinez[46], M. Martini[31], J. Marzec[42], T. Matsubara[6,b], R. Matsumoto[82], M. Matusiak[62], K. Mazurek[62], N. McCauley[55], A. Medhi[61], A. Mefodiev[126], P. Mehta[55], W. J. D. Melbourne[65], L. Mellet[31], D. Mendez-Esteban[44], J. Menendez Maco[33], H. Menjo[99], G. D. Mese Zavala[67], M. Mezzetto[25], J. Migenda[28], P. Migliozzi[30], S. Miki[1], V. Mikola[95], E. Miller[12], A. Minamino[40], S. Mine[1,29], O. Mineev[127], M. Miura[1], R. Moharana[100], C. M. Mollo[30], T. Mondal[101], F. Monrabal[69], C. S. Moon[85], D. H. Moon[86], F. J. Mora Mas[18], L. Morescalchi[93], S. Moriyama[1], Th. A. Mueller[22], T. Nakadaira[6,b], K. Nakagiri[1], M. Nakahata[1], S. Nakai[13], Y. Nakajima[4], K. Nakamura[6], K. D. Nakamura[16], Y. Nakano[102], T. Nakaya[15], S. Nakayama[1], L. Nascimento Machado[95], C. Naseby[12], W. H. Ng[65], K. Niewczas[34], K. Ninomiya[99], S. Nishimori[6,f], Y. Nishimura[76,87], Y. Noguchi[1], T. Nosek[63], F. Nova[43], L. Nožka[53], J. C. Nugent[12], H. Nunokawa[14], M. Nurek[42], E. O'Connor[103], M. O'Flaherty[37], H. M. O'Keeffe[7], E. O'Sullivan[104], W. Obrębski[42], P. Ochoa-Ricoux[29], T. Ogitsu[6,b], R. Okazaki[76], K. Okumura[81,84], N. Onda[15], F. Orozco-Luna[59], N. Ospina[10], M. Ostrowski[105], N. Otani[15], Y. Oyama[6,b], M. Y. Pac[50], P. Paganini[22], J. Palacio[44], M. Pari[25,26], J. Park[85], J. Pasternak[12], C. Pastore[10], G. Pastuszak[42], C. Pate[90], M. Pavin[56], D. Payne[55], J. Pelegrin Mosquera[69], C. Peña-Garay[44], P. de Perio[84], L. Périssé[2], J. Pinzino[93], B. Piotrowski[42], S. Playfer[28], B. Pointon[19,56,106], E. Ponticelli[60], A. Popov[128], B. Popov[31], M. Posiadala-Zezula[107], G. Pronost[1], N. W. Prouse[12,56], C. Quach[22], B. Quilain[2,22], E. Radicioni[10], P. Rajda[108], E. Ramos Cascón[69], R. Ramsden[28], J. Renner[57], M. Rescigno[11], G. Ricciardi[30,60], B. Richards[37], K. Richards[43], D. W. Riley[95], J. Rimmer[89], S. Rodriguez Cabo[33], R. Rogly[22], E. Roig-Tormo[44], M. F. Romo-Fuentes[67], E. Rondio[62], B. Roskovec[63], S. Roth[109], C. Rott[110], A. Rubbia[9], A. C. Ruggeri[30], S. Russo[31], A. Rychter[42], D. Ryu[91], W. Saenz[31], K. Sakashita[6,b,f], S. Samani[35], F. Sánchez[35], M. L. Sánchez Rodríguez[33], E. Sandford[55], A. Santos[22], J. D. Santos Rodríguez[33], A. Sarker[61], P. Sarmah[49], K. Sato[1], Y. Sato[79], C. Schloesser[35], M. Scott[12], Y. Seiya[111], T. Sekiguchi[6,b], H. Sekiya[1,84], J. W. Seo[92], D. Sgalaberna[9], I. Shimizu[115], K. Shimizu[1], C. D. Shin[86], M. Shinoki[79], M. Shiozawa[1], A. Shvartsman[129], A. Simonelli[30], N. Skrobova[130], K. Skwarczynski[62], Benjamin R. Smithers[56], M. Smy[29], J. Sobczyk[34], H. W. Sobel[29], F. J. P. Soler[95], M. S. Sozzi[93,94], R. Spina[10,24], B. Spisso[30], P. Spradlin[95], K. Stankevich[1], D. Stavropoulos[64], L. Stawarz[105], P. Stowell[8], A. Studenikin[131], S. L. Suárez Gómez[33], M. Suchenek[54], Sunanda[100], Y. Suwa[4,15], A. Suzuki[80], S. Y. Suzuki[6], Y. Suzuki[1], D. Svirida[132], M. Tada[6,b], S. Taghayor[56,89], A. Takeda[1], Y. Takemoto[1], A. Taketa[13], Y. Takeuchi[80], V. Takhistov[6,84], H. Tanaka[1], H. K. M. Tanaka[13], M. Tanaka[6], H. Tanigawa[76], T. Tashiro[81], K. Terada[82], M. Thiesse[8], E. Thrane[112], D. Tiwari[19], J. F. Toledo Alarcón[18], A. K. Tomatani Sánchez[67], T. Tomiya[81], N. Tran[15], J. Tseng[20], R. Tsuchii[82], K. M. Tsui[84], T. Tsukamoto[6,b], T. Tsushima[15], M. Tzanov[90], Y. Uchida[12], S. Urano[16], P. Urquijo[65], M. Vagins[84], S. Valder[43], O. Vallmajó[96], G. Vasseur[32], B. Vinning[37], U. Virginet[31], D. Vivolo[30,73], T. Vladisavljevic[43], R. Vogelaar[97], M. Vyalkov[1], T. Wachala[21], D. Wark[20], R. Wendell[15], J. R. Wilson[28], S. Wilson[8], M. Wojciechowski[62], S. Wronka[62], J. Wuethrich[9], J. Xia[84], Z. Xie[28], Y. Yamaguchi[82], K. Yamamoto[111], M. Yamashita[99], K. Yamauchi[79], B. S. Yang[86], T. Yano[1], N. Yershov[133], U. Yevarouskaya[31], M. Yokoyama[4], J. Yoo[113], T. Yoshida[79], Y. Yoshimoto[4], Y. Yoshioka[99], S. Yousefnejad[19], I. Yu[92], T. Yu[56], O. Yuriy[17], B. Zaldivar[68], J. Zalipska[62], K. Zaremba[42], G. Zarnecki[21], X. Zhao[9], H. Zhong[80], T. Zhu[12], M. Ziembicki[54], K. Zietara[105], M. Zito[31,32], S. Zsoldos[28]

[1] Kamioka Observatory, Institute for Cosmic Ray Research, University of Tokyo, Kamioka, Hida, Gifu 506-1205, Japan
[2] ILANCE, CNRS-University of Tokyo International Research Laboratory, Kashiwa, Chiba 277-8582, Japan
[3] Faculty of Sciences, Mohammed V University, Rabat, Morocco
[4] Department of Physics, University of Tokyo, 7-3-1 Hongo, Bunkyo-ku, Tokyo 113-0033, Japan
[5] University of Winnipeg, 515 Portage Ave, Winnipeg, MB R3B 2E9, Canada
[6] High Energy Accelerator Research Organization (KEK), 1-1 Oho, Tsukuba, Ibaraki 305-0801, Japan
[7] Physics Department, Lancaster University, Lancaster LA1 4YB, UK
[8] Department of Mathematical and Physical Sciences, Western Bank, University of Sheffield, Sheffield S10 2TN, UK
[9] Institute for Particle Physics and Astrophysics, ETH Zurich, Otto-Stern-Weg 5, 8093 Zurich, Switzerland

[10] INFN Sezione di Bari, via Orabona 4, 70126 Bari, Italy
[11] INFN Sezione di Roma, P.le A.Moro 2, 00185 Rome, Italy
[12] Department of Physics, Blackett Laboratory, South Kensington Campus, Imperial College London, London SW7 2AZ, UK
[13] Earthquake Research Institute, The University of Tokyo, 1-1-1 Yayoi, Bunkyo-ku, Tokyo 113-0032, Japan
[14] Department of Physics, Pontifícia Universidade Católica do Rio de Janeiro (PUC-Rio), Rua Marquês de São Vicente, 225, Gávea, Rio de Janeiro 22451900, Brazil
[15] Department of Physics, Kyoto University, Kyoto 606-8502, Japan
[16] Faculty of Science, Tohoku University, Aoba, Aramaki, Aoba-ku, Sendai 980-8578, Japan
[17] Kyiv National University, Kyiv, Ukraine
[18] Universitat Politècnica de València (UPV), ETSIT, Camino de Vera, s/n., 46022 Valencia, Spain
[19] Department of Physics, University of Regina, 3737 Wascana Parkway, Regina S4S0A2, Canada
[20] Department of Physics, Clarendon Laboratory, University of Oxford, Parks Road, Oxford OX1 3PU, UK
[21] The Henryk Niewodniczanski Institute of Nuclear Physics Polish Academy of Sciences, ul. Radzikowskiego 152, 31-342 Kraków, Poland
[22] Laboratoire Leprince-Ringuet, Ecole Polytechnique, IN2P3-CNRS, 91120 Palaiseau, France
[23] Faculty of Sciences Ain Chock, Hassan II University of Casablanca, Physics, Km 8 Route d'El Jadida, Maarif, B.P. 5366, 20100 Casablanca, Morocco
[24] Politecnico di Bari, via Orabona 4, 70126 Bari, Italy
[25] INFN, Sezione di Padova, via Marzolo 8, 35131 Padua, Italy
[26] Department of Physics and Astronomy, Università di Padova, via Marzolo 8, 35131 Padua, Italy
[27] Department of Physics, York University, 4700 Keele Street, Toronto, ON M3J1P3, Canada
[28] Department of Physics, King's College London, Strand, London WC2R 2LS, UK
[29] Department of Physics and Astronomy, University of California, Irvine 92697-4575, USA
[30] INFN Sezione di Napoli, Via Vicinale Cupa Cintia, 26, 80126 Naples, Italy
[31] Laboratoire de Physique Nucléaire et de Hautes Energies (LPNHE), CNRS/IN2P3, Sorbonne Université, Paris, France
[32] Université Paris-Saclay, Gif-sur-Yvette, France
[33] MOMA Group, Universidad de Oviedo, C. San Francisco, 3, 33003 Oviedo, Asturias, Spain
[34] Wrocław University, Plac Maxa Borna 9, 50-204 Wrocław, Poland
[35] Universite de Geneve, DPNC, 24, quai Ernest-Ansermet, 1211 Geneva 4, Switzerland
[36] S. N. Bose National Centre for Basic Sciences, Kolkata, India
[37] University of Warwick, Physics, Gibbet Hill Road, Coventry CV312NY, UK
[38] Dipartimento di Fisica, Università degli Studi di Salerno, Via Giovanni Paolo II 132, 84084 Fisciano, Italy
[39] INFN Gruppo Collegato di Salerno, Via Giovanni Paolo II 132, 84084 Fisciano, Italy
[40] Department of Physics, Yokohama National University, 79-5 Tokiwadai, Hodogaya-ku, Yokohama, Kanagawa 240-8501, Japan
[41] A. Chełkowski Institute of Physics, Faculty of Science and Technology, University of Silesia in Katowice, ul. Bankowa 12, 40-007 Katowice, Poland
[42] Institute of Radioelectronics and Multimedia Technology, Warsaw University of Technology, Nowowiejska 15/19, 00-665 Warsaw, Poland
[43] STFC Rutherford Appleton Laboratory, RAL PPD and TD, Harwell Science Campus, Didcot OX11 0QX, UK
[44] Canfranc Underground Laboratory (LSC), Paseo de los Ayerbe s/n, 22888 Canfranc, Spain
[45] Institute For Interdisciplinary Research in Science and Education, International Center of Interdisciplinary Science and Education, 07 Science Avenue, Quy Nhon Nam Ward, Quy Nhon, Gia Lai 55131, Vietnam
[46] Institut de Física d'Altes Energies (IFAE)-The Barcelona Institute of Science and Technology (BIST), Campus UAB, 08193 Bellaterra, Barcelona, Spain
[47] Centre for Astroparticles and High Energy Physics (CAPA), University of Zaragoza, C/ Pedro Cerbuna 12, 50009 Zaragoza, Spain
[48] Department of Physics, Faculty of Sciences, Ibn-Tofail University, Kenitra, Campus Universitaire, PB 133, 14000 Kenitra, Morocco
[49] Indian Institute of Technology-Guwahati, Guwahati, India
[50] Laboratory for High Energy Physics, Dongshin University, Naju, Chonnam 58245, Republic of Korea
[51] Department of Physics, School of Engineering Sciences, KTH Royal Institute of Technology, 10691 Stockholm, Sweden
[52] Tecnologico de Monterrey, Escuela de Ingenieria y Ciencias, Blvd. Pedro Infante 3773, 80100 Culiacán, Sinaloa, Mexico
[53] Faculty of Science, Joint Laboratory of Optics, Palacký University Olomouc, 17. listopadu 50A, 772 07 Olomouc, Czech Republic
[54] Nicolaus Copernicus Astronomical Centre of the Polish Academy of Sciences, Astrocent, Rektorska 4, 00-614 Warsaw, Poland
[55] Department of Physics, University of Liverpool, Liverpool L69 7ZX, UK
[56] TRIUMF, 4004 Wesbrook Mall, Vancouver V6T 2A3, Canada
[57] Instituto Galego de Física de Altas Enerxías (IGFAE), Universidade de Santiago de Compostela, Rúa de Xoaquín Díaz de Rábago, s/n, 15705 Santiago de Compostela, Spain
[58] Departamento de Física, CUCEI, Universidad de Guadalajara, Blvd. Marcelino García Barragán 1421, 44430 Guadalajara, Jalisco, Mexico
[59] Doctorado en Tecnologías de la Información, CUCEA, Universidad de Guadalajara, Periférico Norte 799, Los Belenes, 45100 Zapopan, Jalisco, Mexico
[60] Università Federico II di Napoli, Via Vicinale Cupa Cintia, 26, 80126 Naples, Italy
[61] Physics, Tezpur University, Napaam, Sonitpur, Assam 784028, India
[62] National Centre for Nuclear Research, ul. Soltana 7, 05-400 Otwock, Poland
[63] IPNP, FMF Charles University, Ke Karlovu 3, 121 16 Prague 2, Czech Republic
[64] Institute of Nuclear and Particle Physics, NCSR Demokritos, Neapoleos Str. 27 and Patr. Grigoriou E, 15341 Agia Paraskevi, Attiki, Greece
[65] School of Physics, The University of Melbourne, Melbourne, VIC 3010, Australia
[66] Department of Physics, Carleton University, 1125 Colonel By Drive, Ottawa, ON K1S 5B6, Canada
[67] Tecnologico de Monterrey, Escuela de Ingeniería y Ciencias, Ave. Eugenio Garza Sada 2501 Sur Col: Tecnologico, 64700 Monterrey, NL, Mexico

[68] Department of Theoretical Physics and CIAFF, Ciudad Universitaria de Cantoblanco, University Autonoma Madrid (UAM), 28049 Madrid, Spain
[69] Donostia International Physics Center, C/ Manuel Mendizabal 4, 20018 Donostia-San Sebastián, Spain
[70] Oskar Klein Centre and Department of Physics, Stockholm University, 10691 Stockholm, Sweden
[71] Miyagi University of Education, 149 Aramaki-aza-Aoba, Aoba-ku, Sendai 980-0845, Japan
[72] Vishwakarma Institute of Information Technology, S. No. 3/4, Kondhwa (Bk), Pune 411048, India
[73] Università della Campania L. Vanvitelli, Naples, Italy
[74] Mohammed VI Polytechnic University, Ben Guerir, Morocco
[75] Institute for Theoretical Physics and Modeling, Halabyan Street, 34/1, 0036 Yerevan, Armenia
[76] Faculty of Science and Technology, Keio University, Hiyoshi 3-14-1, Yokohama 223-8522, Japan
[77] University of Wisconsin-Madison, Madison, USA
[78] Department of Physics, Okayama university, 3-1-1 Tsushima-naka, Kita-ku, Okayama 700-8530, Japan
[79] Tokyo University of Science, Physics and Astronomy, 2641 Yamazaki, Noda, Chiba 278-8510, Japan
[80] Department of Physics, Graduate School of Science, Kobe University, 1-1 Rokkodai, Nada, Kobe, Hyogo 657-8501, Japan
[81] Research Center for Cosmic Neutrinos, Institute for Cosmic Ray Research, University of Tokyo, 5-1-5 Kashiwa-no-ha, Kashiwa, Chiba 277-8582, Japan
[82] Institute of Science Tokyo, 2-12-1 Ookayama, Meguro-ku, Tokyo 152-8551, Japan
[83] Gwangju Institute of Science and Technology, Physics and Photon Science, 123 Cheomdangwagi-ro, Buk-gu, Gwangju 61005, Republic of Korea
[84] Kavli IPMU/UTokyo, Kavli Institute for the Physics and Mathematics of the Universe (WPI), The University of Tokyo Institutes for Advanced Study, University of Tokyo, Kashiwa, Chiba 277-8583, Japan
[85] Department of Physics, Kyungpook National University, 80 Daehak-ro, Buk-gu, Daegu 41566, Republic of Korea
[86] Chonnam National University, 77, Yongbong-ro, Buk-gu, Gwangju 61186, Republic of Korea
[87] Institute for Cosmic Ray Research, University of Tokyo, Tokyo, Japan
[88] Tokyo Metropolitan University, 1-1 Minamioosawa, Hachioji, Tokyo 192-0397, Japan
[89] Department of Physics and Astronomy, University of Victoria, 3800 Finnerty Road, Victoria V8P 5C2, Canada
[90] Physics and Astronomy, Louisiana State University, 202 Nicholson Hall, Baton Rouge, LA 70803, USA
[91] Physics, Ulsan National Institute of Science and Technology (UNIST), 50 UNIST-gil, Ulju-gun, Ulsan 44919, Republic of Korea
[92] Department of Physics, Sungkyunkwan University, Jangan-gu, Seobu-ro 2066, Suwon 16419, Republic of Korea
[93] INFN Sezione di Pisa, Largo B. Pontecorvo 3, 56127 Pisa, Italy
[94] Dipartimento di Fisica, Università di Pisa, Largo B. Pontecorvo 3, 56127 Pisa, Italy
[95] School of Physics and Astronomy, University of Glasgow, Glasgow G12 8QQ, UK
[96] Mechanical Engineering, University of Girona-AMADE, Carrer Universitat de Girona 4, 17003 Girona, Spain
[97] Virginia Tech, Blacksburg, VA 24060, USA
[98] Physics, University of Toronto, 60 St. George St., Toronto, ON M5S1A7, Canada
[99] Institute for Space-Earth Environmental Research, Nagoya University, Furocho, Chikusa-ku, Nagoya, Aichi 464-8602, Japan
[100] Indian Institute of Technology-Jodhpur, Jodhpur, India
[101] Department of Physics, Indian Institute of Technology-Kharagpur, Kharagpur, West Bengal 721302, India
[102] Faculty of Science, The University of Toyama, Gofuku 3190, Toyama 930-8555, Japan
[103] Oskar Klein Centre and Department of Astronomy, Stockholm University, 10691 Stockholm, Sweden
[104] Department of Physics and Astronomy, Uppsala University, Box 516, 75120 Uppsala, Sweden
[105] Astronomical Observatory, Jagiellonian University, ul. Orla 171, 30-244 Kraków, Poland
[106] Physics, British Columbia Institute of Technology (BCIT), 3700 Willingdon Ave., Burnaby, BC V5G 3H2, Canada
[107] Faculty of Physics, University of Warsaw, Warsaw, Poland
[108] Institute of Electronics, AGH University of Krakow, al. Mickiewicza 30, 30-059 Kraków, Poland
[109] III. Physikalisches Institut, RWTH Aachen University, Sommerfeldstr. 16, 52074 Aachen, Germany
[110] Department of Physics and Astronomy, University of Utah, Salt Lake City, UT 84112, USA
[111] Department of Physics, Osaka Metropolitan University, Osaka 558-8585, Japan
[112] ARC Centre of Excellence for Gravitational Wave Discovery, Monash University, Clayton, VIC 3800, Australia
[113] Department of Physics and Astronomy, Seoul National University, Seoul 08826, Korea
[114] INFN Laboratori Nazionali di Legnaro, Legnaro, Italy
[115] Research Center for Neutrino Science, Tohoku University, 6-3, Aramaki Aza Aoba, Aobaku, Sendai 980-8578, Japan
[116] URL: http://orcid.org/0000-0003-3358-9635
[117] URL: http://orcid.org/0000-0001-9227-5164
[118] URL: http://orcid.org/0000-0002-5696-4234
[119] URL: http://orcid.org/0000-0002-7495-6860
[120] URL: http://orcid.org/0000-0002-8446-2362
[121] URL: http://orcid.org/0000-0001-5428-0464
[122] URL: http://orcid.org/0000-0003-4234-2079
[123] URL: http://orcid.org/0000-0002-4835-2270
[124] URL: http://orcid.org/0000-0002-1624-6131
[125] URL: http://orcid.org/0000-0003-3204-9426
[126] URL: http://orcid.org/0000-0003-1243-0115
[127] URL: http://orcid.org/0000-0001-6550-4910
[128] URL: http://orcid.org/0000-0002-4715-2373
[129] URL: http://orcid.org/0000-0002-7160-2549

[130] URL: http://orcid.org/0000-0003-0783-6655
[131] URL: http://orcid.org/0000-0003-3310-9072
[132] URL: http://orcid.org/0000-0002-0334-7304
[133] URL: http://orcid.org/0000-0002-7405-1770

Received: 20 May 2025 / Accepted: 13 October 2025

Abstract This paper presents the expected sensitivity to the neutrino oscillation parameters of the Hyper-Kamiokande long-baseline program. The Hyper-Kamiokande experiment, currently under construction in Japan, will measure the oscillations of accelerator-produced neutrinos with thousands of selected events per sample: this corresponds to an increase of statistics of a factor 25–100 with respect to recent results from the currently-running long-baseline neutrino oscillation experiment in Japan, T2K. In the most favorable scenario we will achieve the discovery of Charge-Parity (CP) violation in neutrino oscillation at 5σ C.L. in less than 3 years. With 10 years of data-taking, and assuming a neutrino : antineutrino beam running ratio of 1:3, a CP violation discovery at 5σ C.L. is possible for more than 60% of the actual values of the CP-violating phase, δ_{CP}. Moreover, we will measure δ_{CP} with a precision ranging from 20°, in the case of maximal CP violation, to 6°, in the case of CP conservation. We aim to achieve a 0.5% resolution on the Δm^2_{32} parameter, and a resolution between 3% and 0.5% on the $\sin^2\theta_{23}$ parameter, depending on its true value. These results are obtained by extending the analysis methods of T2K with dedicated tuning to take into account the Hyper-Kamiokande design: the larger far detector, the more powerful beam, the upgraded near detector ND280, and the planned additional Intermediate Water Cherenkov Detector.

1 Introduction

Neutrinos propagate as mass eigenstates (ν_1, ν_2, ν_3), while they interact with matter as flavour eigenstates of the weak interaction (ν_e, ν_μ, ν_τ), coupling to the corresponding charged leptons (electron, muon and tau). In the standard paradigm of neutrino oscillations, the three mass eigenstates can be expressed as an admixture of the flavour eigenstates using a 3×3 unitary mixing matrix ($U_{\alpha k}; \alpha = e, \mu, \tau; k = 1, 2, 3$), so called Pontecorvo–Maki–Nakagawa–Sakata (PMNS) [1,2] matrix. If neutrinos are Dirac particles, out of the nine degrees of freedom of such a matrix, five could be reabsorbed as unphysical phases in the definition of the lepton fields. In the most used parametrization [3] the remaining degrees of freedom are encoded in a SO(3) matrix, using Tait–Bryan rotation angles (θ_{12}, θ_{13}, and θ_{23}), and an additional complex phase δ_{CP}, which parameterizes a possible Charge-Parity violation (CPV) in the lepton sector. Considering the time evolution of the mass eigenstates during their propagation, the neutrino oscillation probability also depends on the squared mass difference between the pairs of mass eigenstates ($\Delta m^2_{ij} = m^2_i - m^2_j$).

In this paper we present the sensitivity of the Hyper-Kamiokande experiment to measuring the oscillation parameters using accelerator neutrinos. As of today, all three mixing angles, as well as the Δm^2_{21} and $|\Delta m^2_{32}|$ parameters have been measured with a few percent precision or better [3]. The phase δ_{CP} is still unknown, first hints from T2K [4] point to large CPV, but they are not confirmed by NOvA [5]. A possible definitive discovery of this new fundamental source of CPV, the first in the lepton sector, would have profound implications on the comprehension of the matter–antimatter asymmetry in the Universe, in particular in the framework of leptogenesis [6] with low-energy seesaw mechanisms [7]. CPV discovery is the primary target of the Hyper-Kamiokande sensitivity analysis reported in this paper. The sign of Δm^2_{32}, also known as the mass ordering (MO), is still unknown, with first indications from Super-Kamiokande [8] atmospheric neutrino measurements showing a preference for normal ordering ($m_3 > m_2$). The octant of the θ_{23} mixing angle is still unknown, and maximal mixing between muon and tau neutrinos ($\theta_{23} = \pi/4$) is possible. In the next decade these neutrino oscillation parameters will be also measured by another long-baseline experiment, DUNE [9], in construction in US.

From a broader perspective, the present oscillation paradigm consists of an effective parametrization of flavour mixing: whether or not the specific values of the oscillation parameters are due to an underlying fundamental symmetry or an underlying basic principle remains an open question. Precise measurements of these parameters, within the scope of the

[a] Now at the University of Warsaw, Warsaw, Poland
[b] Also at J-PARC, Naka, Ibaraki, Japan
[c] Also at Université Paris-Saclay, Gif-sur-Yvette, France
[d] Also at Departament de Fisica de la Universitat Autonoma de Barcelona, Barcelona, Spain
[e] Also at Qilimanjaro Quantum Tech S.L., Carrer de Veneçuela, 74, 08019 Barcelona, Spain
[f] Also at SOKENDAI, Tsukuba, Japan
[g] Also at Kobayashi-Maskawa Institute for the Origin of Particles and the Universe, Nagoya University, Nagoya, Japan
[h] Also at CIRA, the Italian Aerospace Research Centre, Capua 81043, Italy

[a] e-mail: hyperkpb@km.icrr.u-tokyo.ac.jp (corresponding author)

present Hyper-Kamiokande analysis, may hint at, or at least help to discard, specific flavour symmetry models [10].

1.1 The Hyper-Kamiokande experiment

Hyper-Kamiokande [11,12] is an experiment under construction aiming to perform precision measurements of neutrino oscillations and determine whether neutrinos violate Nature's CP symmetry. It will also perform the world's most sensitive search for proton decay, supernova neutrinos detection and other physics measurements. Hyper-Kamiokande will start data taking in 2028 and is the third-generation water Cherenkov neutrino detector in Japan, following Kamiokande [13] and Super-Kamiokande [14], the experiment currently underway. Hyper-Kamiokande will measure oscillations of atmospheric and solar neutrinos as well as oscillations of neutrinos produced by an accelerator, as in its predecessor long-baseline experiments K2K (KEK to Kamioka) [15] and T2K (Tokai to Kamioka) [16].

The Hyper-Kamiokande experiment consists of the existing J-PARC neutrino beam and a set of near detectors, both currently used for the T2K experiment and being upgraded to increase performance, and two new water Cherenkov detectors, an intermediate detector of about 600-ton at around 1 km from the neutrino beam production target and a 258,000-ton far detector at 295 km (oscillation baseline).

The J-PARC accelerator complex provides a beam of 30 GeV protons and is being upgraded to reach 1.3 MW power near the beginning of the Hyper-Kamiokande data taking [17]. The proton beam impinges on a graphite target, producing hadrons (primarily pions and kaons) which are focused and charge-selected by three electromagnetic horns. The hadrons are thus guided to a 96 m long He-filled vessel, where they decay generating a flux of charged leptons and neutrinos. The produced neutrino flux is highly dominated by muon neutrinos, with a small background ($< 1\%$) of electron neutrinos. A flux dominated by neutrinos (Forward Horn Current, FHC) or antineutrinos (Reverse Horn Current, RHC) can be produced by inverting the polarity of the horns. Hyper-Kamiokande will rely on the off-axis technique, which profits from the kinematic properties of the two-body pion decay: by placing the near and far detectors at 2.5° off of the beam axis, the neutrino energy is peaked at 600 MeV, corresponding to maximal neutrino oscillations at a propagation baseline of 295 km, while the fraction of beam electron neutrinos, mostly coming from muon and kaon decays, is reduced.

The Hyper-Kamiokande far detector will be built 295 km from the production target and situated beneath the peak of Mt. Nijyugo, resulting in a 1750 ms-water-equivalent overburden. The detector is a 71 m high and 68 m diameter cylinder filled with ultra-pure water and split into optically isolated inner and outer detector regions. The outer detector (OD) will consist of a shell surrounding the inner detector. The OD is 1 m wide in the vertical barrel and 2 m tall at the top and bottom caps. The OD will be instrumented with approximately 3600 8 cm diameter photomultiplier tubes (PMTs), each equipped with a 30 cm $\times$ 30 cm wavelength shifting plate to enhance light collection. The outer detector will identify and veto entering charged particles, such as cosmic muons or particles created by neutrino interactions in the surrounding rock. The inner detector, acting as main target for the neutrino interactions, has a volume of about 217 kton and will be instrumented with approximately 20,000 50 cm diameter PMTs and 1000 multi-PMT photosensor modules. The photo-cathode coverage of Hyper-Kamiokande will be about 20%, compared to 40% at Super-Kamiokande. However, the light collection efficiency of the 50 cm PMTs is doubled. The photon detection efficiency of Hyper-Kamiokande will therefore be approximately equal to that of Super-Kamiokande. A detailed description of the Hyper-Kamiokande far detector could be found in Ref. [12].

The set of near detectors placed 280 m from the beam target includes INGRID [18], located on-axis for beam position and direction monitoring, and ND280, a magnetized multipurpose detector which measures the neutrino flux and neutrino-nucleus interaction cross-sections. The ND280 detector has been recently upgraded [19] to increase the detectable kinematic range of particles from neutrino interactions, in view of the additional statistics still to be collected by the T2K experiment. The upgraded ND280 detector will also serve the Hyper-Kamiokande experiment. ND280 consists of two main tracking regions: two vertical targets composed of sets of perpendicular scintillating bars (one target also hosting bags of passive water) interleaved with three vertical Time Projections Chambers; and a horizontal, highly granular, scintillator detector sandwiched between two horizontal Time Projection Chambers and further surrounded by scintillating panels for Time of Flight measurement. The detectors are surrounded by an electromagnetic calorimeter and embedded into a 0.2 T magnet, which also hosts a muon range detector. A detailed description of the upgraded ND280 detector could be found in Ref. [19].

Alongside the upgraded ND280, a new water Cherenkov detector will be built approximately 1 km from the neutrino production target [12]. The Intermediate Water Cherenkov Detector (IWCD) preliminary design consists of an 8.8 m diameter and 10 m tall cylinder with a 7 m diameter and 8 m tall inner detector region. The inner detector will be instrumented with about 350 multi-PMT modules and will have a target mass of approximately 300 tonnes. The detector will be placed in a vertical pit allowing the detector to be positioned anywhere between 4° and 1.5° off the central axis of the neutrino beam. IWCD can directly measure the relationship between true and reconstructed neutrino energy by sampling different off-axis angles [20]. The large target mass, high precision electron/muon discrimination and self-

shielding property of water also allow IWCD to make precise measurements of electron neutrino and antineutrino cross-sections.

1.2 Neutrino oscillation probabilities

The Hyper-Kamiokande accelerator neutrino flux is peaked at about 600 MeV, an energy where matter effects are subdominant ($< 10\%$). While the oscillation formulas used in the analysis described here correctly include matter effects, oscillation formulas in vacuum will be described in this section as a simplified paradigm to show the sensitivity of the various Hyper-Kamiokande samples to the oscillation parameters. We can consider four main channels: muon (anti)neutrino disappearance and electron (anti)neutrino appearance. While most muon (anti)neutrinos oscillate into tau (anti)neutrinos, tau production from charged-current interactions is possible only in the high-energy tail of the Hyper-Kamiokande (anti)neutrino flux, thus far from the oscillation maximum. For this reason this sample is not considered in this paper.

The muon (anti)neutrino disappearance formula in vacuum, relying on the PMNS parametrization of the mixing matrix, reads

$$P(\overset{(-)}{\nu}_\mu \to \overset{(-)}{\nu}_\mu) \simeq 1 - \sin^2 2\theta_{23} \sin^2\left(1.27\frac{\Delta m^2_{32} L}{E}\right), \quad (1)$$

with L as the oscillation baseline, in km, E as the neutrino energy, in GeV, and Δm^2_{32} in eV^2. The formula is independent on δ_{CP}, thus applies to both neutrino and antineutrino disappearance in the standard oscillation paradigm. Exotic oscillation scenarios based on new physics models [21], such as CPT violation through comparisons of muon neutrino and antineutrino oscillation probabilities, are not covered in this study. As can be seen from Eq. 1, the muon (anti)neutrino samples are sensitive to the so-called atmospheric parameters, $|\Delta m^2_{32}|$ and $\sin^2 2\theta_{23}$. On the other hand, these samples cannot measure the sign of Δm^2_{32}, i.e. the MO, and they suffer from a degeneracy of the θ_{23} octant, i.e. cannot distinguish $[0, \pi/4]$ from $[\pi/4, \pi/2]$. We can resolve this degeneracy using electron (anti)neutrino appearance samples. The formula for electron (anti)neutrino appearance in vacuum, in the $\Delta m^2_{21}/\Delta m^2_{31} \ll 1$ approximation, is

$$\begin{aligned} P(\overset{(-)}{\nu}_\mu \to \overset{(-)}{\nu}_e) \simeq\ & 4c^2_{13}s^2_{13}s^2_{23} \cdot \sin^2\Delta_{31} \\ & + 8c^2_{13}s_{12}s_{13}s_{23}(c_{12}c_{23}\cos\delta_{CP} - s_{12}s_{13}s_{23}) \\ & \cdot \cos\Delta_{32} \cdot \sin\Delta_{31} \cdot \sin\Delta_{21} \\ & - (+)8c^2_{13}c_{12}c_{23}s_{12}s_{13}s_{23}\sin\delta_{CP} \cdot \sin\Delta_{32} \cdot \sin\Delta_{31} \cdot \sin\Delta_{21} \\ & + 4c^2_{13}s^2_{12}(c^2_{12}c^2_{23} + s^2_{12}s^2_{13}s^2_{23} - 2c_{12}c_{23}s_{12}s_{13}s_{23}\cos\delta_{CP}) \\ & \cdot \sin^2\Delta_{21}, \end{aligned} \quad (2)$$

where we shortened $s_{ij} = \sin\theta_{ij}$, $c_{ij} = \cos\theta_{ij}$, $\Delta_{ij} = 1.27\Delta m^2_{ij}L/E$ (same units as Eq. 1) and the term depending on $\sin\delta_{CP}$ is CP-odd, thus changing sign for antineutrinos. Hyper-Kamiokande will, therefore, feature a direct sensitivity to the CP asymmetry between neutrino and antineutrino oscillations, notably thanks to the capability of the beamline to produce a clean flux of neutrinos (in FHC) and antineutrinos (in RHC). Inclusion of constraints from solar neutrino measurements [22–27] and KamLAND experiment [28] on the θ_{12} and Δm^2_{21} parameters and from the reactor experiments on the θ_{13} angle [29–31] further enhance such sensitivity.

When considering matter effects in the oscillation equations [32,33], the (anti)neutrino appearance samples also feature a sensitivity to the MO, manifesting itself as an additional asymmetry between electron neutrino and antineutrino appearance probabilities. At the energy of the Hyper-Kamiokande flux, matter effects are minor and they are degenerate with CPV effects, except in the two extreme cases where matter effects push the neutrino/antineutrino asymmetry beyond what is allowed by maximal CPV (notably, $\delta_{CP} = -\pi/2$ and normal ordering or $\delta_{CP} = \pi/2$ and inverted ordering). In Hyper-Kamiokande, the MO will be measured with atmospheric neutrinos: the combination of atmospheric and beam neutrinos [12] reaches between 3.5 and 4.5σ MO determination in 6 years of data taking, depending on the value of $\sin^2\theta_{23}$ in the 1σ interval from presently available oscillation measurements. Indeed, MO can also be measured by other experiments apart from long-baseline approaches: various running and forthcoming atmospheric and reactor experiments [8,34–36] feature high sensitivity to MO. In the following, we will therefore assume that MO is known and is normal. Whenever this assumption could have a sizable impact on the results, e.g. delaying the reach of CPV discovery, we will explicitly mention it.

2 Event simulation

2.1 Assumed exposure

Hyper-Kamiokande is expected to collect statistics from 2.7×10^{21} Protons-On-Target (POT) per calendar year, corresponding to 6 cycles of 22 days with 87% running efficiency at 1.3 MW. We chose a partition of 1/4 of the exposure in FHC and 3/4 in RHC, considering proper control of systematic uncertainties and direct access to extensive statistics of both neutrino and antineutrino events for a robust assessment of CPV. In particular, this FHC/RHC partition is the optimal one to break the CPV degeneracy with $\sin^2\theta_{23}$ and $\sin^2\theta_{13}$. Due to difference in the cross-section and flux of neutrinos and antineutrinos, this partition leads to a comparable num-

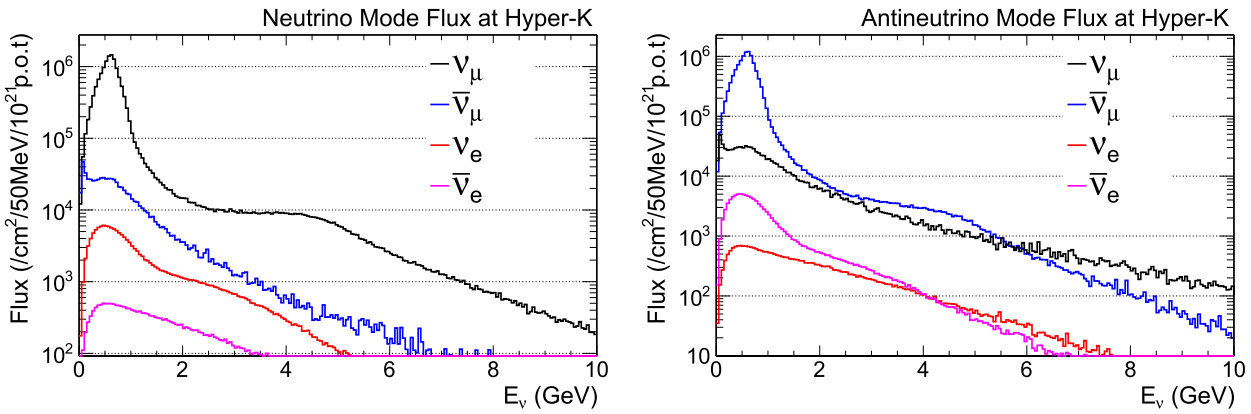

Fig. 1 Simulated flux at the far detector in neutrino mode (left) and antineutrino mode (right)

Table 1 Values of the oscillation parameters assumed for the sensitivity studies, unless specified otherwise

$\sin^2\theta_{12}$	Δm^2_{21}	$\sin^2\theta_{23}$	Δm^2_{32}	$\sin^2\theta_{13}$	δ_{CP}	Mass ordering
0.307	7.53×10^{-5} eV^2	0.528	2.509×10^{-3} eV^2	0.0218	-1.601 rad	Normal

Table 2 Expected number of events at Hyper-Kamiokande with 27×10^{21} POT (6.75×10^{21} POT in FHC and 20.25×10^{21} POT in RHC), corresponding to 10 years of accumulated statistics. The first four columns correspond to non-oscillated events which include electron (anti)neutrinos from the intrinsic beam contamination

	Beam ν_μ	Beam ν_e	Beam $\bar{\nu}_\mu$	Beam $\bar{\nu}_e$	$\nu_\mu \to \nu_e$	$\bar{\nu}_\mu \to \bar{\nu}_e$	Total
ν-mode, 1-ring μ-like	8355.4	8.4	478.0	0.7	2.6	0.01	8845.1
$\bar{\nu}$-mode, 1-ring μ-like	4255.9	6.0	7759.9	4.7	0.2	0.4	12,027.2
ν-mode, 1-ring e-like + 0 decay e	143.9	294.3	5.3	12.0	2007.5	11.7	2474.7
$\bar{\nu}$-mode, 1-ring e-like + 0 decay e	59.1	130.1	96.3	234.8	229.2	793.2	1542.7
ν-mode, 1-ring e-like + 1 decay e	14.0	40.2	0.6	0.3	255.3	0.2	310.6

ber of events in the FHC and RHC electron-like samples in the case of CP symmetry conservation.

We use the neutrino flux model of the T2K experiment [37] as the basis for the analysis shown here. The expected neutrino flux has been weighted to take into account the expected increase in horn current (from 250 kA used in the simulation of the T2K flux to 320 kA for Hyper-Kamiokande) and the different relative position of the far detector (same off-axis angle but on the opposite side of the beam center). The simulated flux is shown in Fig. 1. The initial flux uncertainties (i.e. without any constraint by the near detector) are the same as in Ref. [4], which profit from the NA61/SHINE hadroproduction measurements using the T2K replica target from Ref. [38].

2.2 Event samples

To model the expected event rates and kinematics at the far detector, we use the T2K Monte Carlo simulation. Full details of the simulation, event reconstruction and event selection are described in Ref. [4]. All events must be fully contained in the inner detector and have only one prompt reconstructed particle, an outgoing lepton, in order to enhance the fraction of quasi-elastic events where the neutrino energy can be estimated more accurately. The events are then separated into electron-like (1Re) and muon-like (1Rμ) samples, and a sample-dependent fiducial volume cut is applied. Further cuts are applied to remove background events, such as pions produced by neutral current neutrino interactions. Finally, the electron-like events are required to have a maximum reconstructed neutrino energy of 1.25 GeV, since higher-energy beam neutrinos are insensitive to oscillations and prone to mismodeling of systematic uncertainties. The samples are separated depending on the horn current, between neutrino- (FHC) or antineutrino-dominated (RHC) beam. We include an additional sample of electron-like events that have one delayed triggered signal relative to the primary interaction, consistent with a Michel electron from an unseen, positively-charged pion decay chain (1Re1De). This sample is only included for the FHC beam mode and is mostly populated by events with single pion production.

A scaling has been applied to the generated Monte-Carlo events to take into account the increased size of the Hyper-Kamiokande far detector compared to Super-Kamiokande.

Events are separated according to the distance from the interaction vertex to the tank wall in the lepton's direction of travel (so-called "ToWall" parameter). Events with ToWall larger than 200 cm are scaled by the ratio of the detectors' fiducial volume (≈ 8.3). The remaining events (ToWall smaller than 200 cm) are scaled by the ratio of the surface areas of the detectors (≈ 3.6). This difference in scaling is applied to take into account the fact that the event reconstruction performance is worse for interactions near the wall and the volume/surface ratio is different between Hyper-Kamiokande and Super-Kamiokande. This scaling provides a conservative estimation of the total number of events which is 10% smaller than the full volume ratio.

The size of the simulated samples is large enough to ensure a negligible uncertainty due to Monte-Carlo statistics (between 0.3% and 0.1%, depending on the sample).

Unless specified otherwise, we will assume the value of oscillation parameters reported in Table 1. These are the values usually assumed in T2K validation studies, e.g. in Ref. [4], since they are close to the best fit to T2K data. When relevant, the dependence of the Hyper-Kamiokande sensitivity to the specific value of these oscillation parameters will be studied. We report in Table 2 the number of expected events and their kinematic distributions are shown in Fig. 2. The main kinematic variables considered in the analysis are the momentum and angle of the outgoing lepton: in the muon-like samples we use such observables to reconstruct the neutrino energy using the quasi-elastic assumption [39], enabling more direct sensitivity to the shape of the oscillated energy spectrum. Thus, the fit to the oscillation parameters is performed in lepton angle and momentum (quasi-elastic energy) for the 1Re (1Rμ) sample.

3 Analysis

3.1 Overview

The analysis developed for the T2K experiment [4] is adapted to take into account the different configuration of beam and detectors in Hyper-Kamiokande. The general principles of the analysis are described below.

The uncertainty in the simulated neutrino flux and interaction cross-section models is parameterised. Then, the parameters are fit to near-detector event samples to both tune the model prediction and reduce the uncertainty on the predicted event spectra at the far detector. This tuned model is then fit to the simulated far detector event samples to extract the sensitivity to the neutrino oscillation parameters, while also including uncertainties associated with the far detector reconstruction as nuisance parameters.

3.2 Systematic uncertainties and near detector inputs

We use the neutrino flux, neutrino-nucleus interaction cross-section and detector response models developed by the T2K collaboration and, therefore, adopt the same parameterisation of the model uncertainties. A detailed description of these can be found in Ref. [4].

The systematic uncertainties related to the modeling of the far detector are implemented as a weighting of the number of selected events according to the sample, neutrino interaction type and reconstructed neutrino energy. T2K has constrained these uncertainties using a fit to the Super-Kamiokande atmospheric neutrino samples and other dedicated background control samples.

The flux systematic uncertainties are implemented in terms of binned nuisance parameters which weight the number of expected neutrinos at Hyper-Kamiokande as a function of neutrino type (electron or muon flavour for neutrinos and antineutrinos), beam mode (FHC and RHC) and neutrino energy. Uncertainties are evaluated using NA61/SHINE hadroproduction measurements, beam line modeling and alignment uncertainties, measurements of the horn current, proton beam monitoring data, and measurements from the on-axis neutrino beam monitor INGRID. We assume that Hyper-Kamiokande will achieve a level of beam systematic uncertainties similar to that T2K has demonstrated.

We consider four main types of neutrino-nucleus interactions: charged-current quasi-elastic, interactions with pairs of correlated nucleons (also called 2p2h), single pion production and other interactions (including multi-pion production and deep inelastic scattering). The kinematics, type and number of particles observed in the detector can be further modified by so-called "final state interactions" (FSI) of pions and nucleons as they exit the nucleus. Coulomb corrections to the momenta of charged particles leaving the nucleus are also implemented. Uncertainties on the fundamental physics parameters inside the interaction model are included when technically possible, or otherwise as effective weights in bins of the fundamental kinematic variables (neutrino energy, transferred 4-momentum to the nucleus, among others) or as overall normalization uncertainties for specific processes. These uncertainties are set based on theoretical arguments and neutrino cross-section measurements from the T2K near detectors and other dedicated experiments.

The neutrino flux and cross-section uncertainties will be constrained in Hyper-Kamiokande by a set of near detectors, including the upgraded T2K near detector ND280 and a new Intermediate Water Cherenkov Detector. In this analysis, we consider the constraints obtained by the T2K experiment from ND280 data in Ref. [4], and we assume further improvements on the basis of the expected increase of statistics at Hyper-Kamiokande and of the improved capabilities of upgraded ND280 [40] and IWCD.

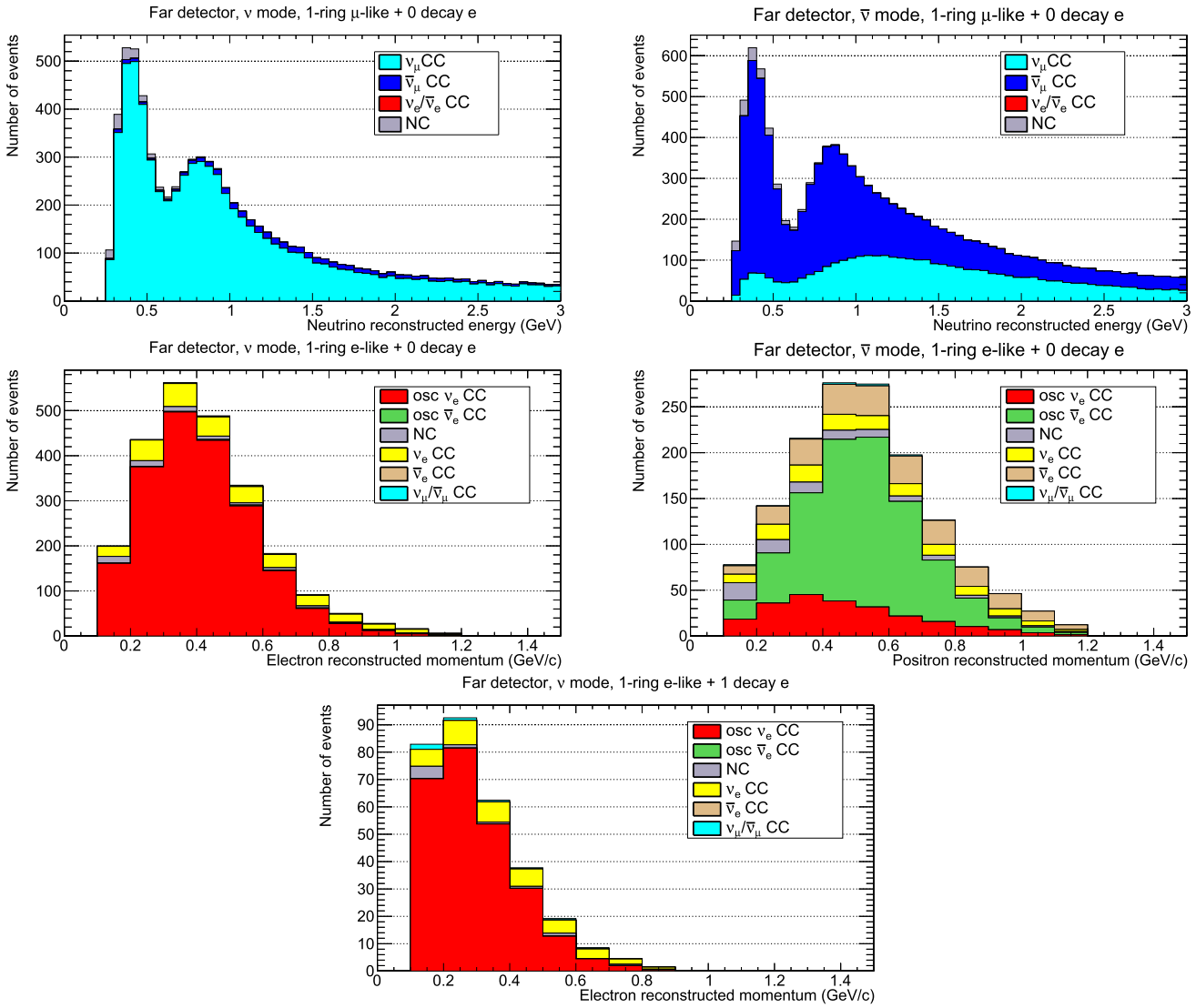

Fig. 2 Reconstructed spectra of the selected samples predicted with 27×10^{21} POT (6.75×10^{21} in FHC and 20.25×10^{21} in RHC), corresponding to 10 years of accumulated statistics. The electron (anti)neutrino samples are separated between appearance neutrinos from oscillation ('osc') and the intrinsic electron neutrino component of the beam.

Table 3 1σ uncertainty on the number of events expected in each sample for each source of uncertainty for either the same systematic errors as the T2K analysis [4] after the near detector fit (T2K syst.) or an improved error model considering 10 years of data accumulated at the near and far detectors (Impr. syst.). The uncertainty on the ratio of 1Re event sample in FHC and RHC is reported in the last column

T2K systematics	FHC 1Re	FHC 1Rμ	RHC 1Re	RHC 1Rμ	FHC 1Re1De	FHC/RHC 1Re
Flux-xsec	3.6%	2.1%	4.3%	3.4%	4.9%	4.4%
Detector	3.1%	2.1%	3.9%	1.9%	13.2%	1.1%
All	4.7%	3.0%	5.9%	4.0%	14.1%	4.6%
Improved systematics	**FHC 1Re**	**FHC 1Rμ**	**RHC 1Re**	**RHC 1Rμ**	**FHC 1Re1De**	**FHC/RHC 1Re**
Flux-xsec	1.8%	0.9%	1.6%	0.9%	1.8%	1.9%
Detector	1.1%	0.8%	1.5%	0.7%	4.9%	0.4%
All	2.1%	1.2%	2.2%	1.1%	5.2%	2.0%

We build the improved systematics prediction by modifying the errors associated with each systematic parameter in the T2K model without modifying the correlations between the parameters. The value of the various uncertainties before rescaling could be found in Ref. [4]. For all parameters constrained by ND280, the uncertainty is scaled by $\sqrt{1/N}$, where N indicates the number of events which is proportional to POT. The ratio of POT between 10 years of Hyper-Kamiokande data taking and the T2K analysis of Ref. [4] (3.6×10^{21} POT) is 7.5. This rescaling relies on the implicit assumption that the final uncertainty from the near detector constraint is limited by the statistics at the near detector and, as a consequence, the near detector systematic uncertainties must be smaller than the statistical error. This assumption is verified in T2K, it is further ensured by the upgraded ND280 and is fundamentally motivated by the fact that systematic uncertainties can be constrained from control samples which increase in statistics at the same pace of the signal samples. We also assume that the near to far detector data-taking ratio will be similar between T2K and Hyper-Kamiokande. Finally, the far detector systematic uncertainties from Ref. [4] are also scaled by the same factor $1/\sqrt{7.5}$ considering 10 years of Hyper-Kamiokande. This is a somewhat arbitrary assumption: the far detector systematic uncertainties will be constrained using calibration sources and various control samples. We assume that the achievable precision will roughly scale with the collected statistics, which increases with the volume change between Hyper-Kamiokande and Super-Kamiokande.

In addition to the reduction due to increased statistics, further reductions to individual parameter uncertainties were applied based on the expected performance of the upgraded ND280 and IWCD detectors. In general, such detectors will feature improved angular acceptance and much increased target mass. The improved reconstruction of the hadronic final state in the upgraded ND280, notably enabling lower threshold for proton reconstruction, is expected to strongly reduce the quasi-elastic uncertainties [40]. In addition, lower pion threshold will further improve the precision of pion-production measurements. In case of neutron production, dominant in antineutrino interactions, the upgraded ND280 will allow for the first time the measurement of neutron kinematics but with somewhat lower efficiency and less precision than for final states with protons [41]. IWCD will provide extremely large statistics samples for both charged and neutral current interactions. The off-axis spanning capability of IWCD provides a direct link between neutrino energy and reconstructed particle kinematics, allowing precise measurements of energy mis-reconstruction and as a result improved constraints on charged current systematic uncertainties, particularly those associated to multi-nucleon and resonant interactions. Water Cherenkov detectors also provide high purity and efficiency samples of neutral current interactions through the reconstruction of neutral pions. On the basis of these considerations, the following reductions of systematic uncertainties have been applied. For charged-current interactions, we have reduced neutrino non-quasi-elastic uncertainties by a factor of three, quasi-elastic uncertainties by a factor of 2.5 and all antineutrino uncertainties by a factor of 2. Uncertainties on neutral current interactions were reduced to $\sim 10\%$. The energy dependent uncertainties on 2p2h are not modified: while the off-axis spanning of IWCD and the improved energy reconstruction capabilities of the upgraded ND280 are expected to improve energy-dependent uncertainties, we defer quantitative evaluation to further studies. The errors on the $\sigma(\nu_e)/\sigma(\nu_\mu)$ and $\sigma(\bar{\nu}_e)/\sigma(\bar{\nu}_\mu)$ cross-section ratios are fixed to 1.7% each, with an anti-correlation of -0.33. The error on the ratio of true-sign $\bar{\nu}_e/\nu_e$ events in the 1Re sample is thus 2.7% (unless specified otherwise).

Theoretical uncertainties on the $\nu_e/\bar{\nu}_e$ interaction cross-section, with respect to the $\nu_\mu/\bar{\nu}_\mu$ cross-section, arise from mis-modeling of nuclear effects and radiative corrections, which depend on the lepton mass difference between electrons and muons in charged-current interactions. The systematic parameters governing the magnitude of these two effects are mostly correlated between ν and $\bar{\nu}$. The impact of $\nu_e/\bar{\nu}_e$ uncertainty in the Hyper-Kamiokande flux and kinematic region is studied in Ref. [42] for the nuclear physics uncertainties and Ref. [43] for the radiative corrections. Both papers study the specific Hyper-Kamiokande kinematic region showing, respectively, that nuclear uncertainties are expected to be below 2% and a kinematic-dependent prediction of radiative corrections gives a residual uncertainty below 0.5%. Such theoretical inputs will be further corroborated by direct measurements at IWCD and upgraded ND280. The 2.7% uncertainty on $\sigma(\nu_e)/\sigma(\bar{\nu}_e)$ is thus a reasonable target in the Hyper-Kamiokande era.

The model of uncertainties developed by the T2K collaboration is very detailed and its robustness has been proven in multiple iterations of T2K data analysis and in dedicated simulated test datasets built using alternative neutrino interaction models. While such a model will certainly be further refined in anticipation of the increased statistical power of both the ongoing T2K and upcoming Hyper-Kamiokande experiments, it is a reasonable, data-driven approach to test the sensitivity of Hyper-Kamiokande. The robustness of the results for very large statistics was tested in various ways. We enforced each single systematic uncertainty to be constrained not better than 1% and obtained stable results, ensuring that they are not dominated by any over-constrained uncertainty. We also tested that in the case of maximal (10 years) far detector statistics, the primary constraint on the model is still coming from the near detectors. Note that unless specified otherwise, the improved systematics prediction is built considering the expected statistical power after 10 years of Hyper-Kamiokande operation.

Table 3 shows the resulting systematic uncertainties on the number of expected events at Hyper-Kamiokande. The two scenarios of "T2K systematics" and "Improved systematics" bracket the level of systematic uncertainties which is expected during the life of the Hyper-Kamiokande experiment, between the start of the experiment up to 10 years of data taking. In the following we report sensitivities for Hyper-Kamiokande using both scenarios, as well as sensitivities assuming statistical errors only. These results highlight the impact that the systematics error model has on the physics reach of Hyper-Kamiokande.

3.3 Fit of the oscillation parameters

The neutrino oscillation parameter sensitivities reported here assume a full three-flavor PMNS parameterization of neutrino mixing. The oscillation parameters δ_{CP}, θ_{23}, and Δm^2_{32} are fit without external constraints, while θ_{13} is fit both without and with a Gaussian external constraint of $\sin^2 2\theta_{13} = 0.0853 \pm 0.0027$ coming from measurements using reactor antineutrinos [3]. The values of $\sin^2\theta_{12} = 0.307$ and $\Delta m^2_{21} = 7.53 \times 10^{-5}$ eV^2 are held fixed in the fit following the measurements from solar and reactor experiments [3].

The analysis is based on a binned maximum likelihood method where the likelihood is defined as:

$$\mathcal{L}(\{N_s^{\text{obs}}, \mathbf{x}_s^{\text{obs}}\}_{\forall s}, \mathbf{o}, \mathbf{f}) = \prod_{s \in \text{samples}} [\mathcal{L}_s(N_s^{\text{obs}}, \mathbf{x}_s^{\text{obs}}, \mathbf{o}, \mathbf{f})] \times \mathcal{L}_{\text{syst}}(\mathbf{f}), \quad (3)$$

where s runs through the samples considered. N_s^{obs} is the number of candidate events observed for sample s and $\mathbf{x}_s^{\text{obs}}$ represent the measurement variables: the electron-like samples are binned into reconstructed charged lepton momentum and scattering angle, while the muon-like samples are binned into reconstructed neutrino energy and charged lepton scattering angle. The symbol $\mathbf{o}$ represents the set of all oscillation parameters we measure, and $\mathbf{f}$ is the set of systematic nuisance parameters. $\mathcal{L}_{\text{syst}}(\mathbf{f})$, the term describing the systematic effects:

$$\mathcal{L}_{\text{syst}}(\mathbf{f}) = \exp\left(-\frac{(\mathbf{f}-\mathbf{f_0})^T V^{-1} (\mathbf{f}-\mathbf{f_0})}{2}\right), \quad (4)$$

where $\mathbf{f_0}$ is the set of prior preferred values of the systematic parameters and V is the covariance matrix that describes the input uncertainty on the systematic parameters and their correlations. This frequentist analysis is performed with the same fitting framework of Ref. [4] and all nuisance (systematic and oscillation) parameters are profiled.

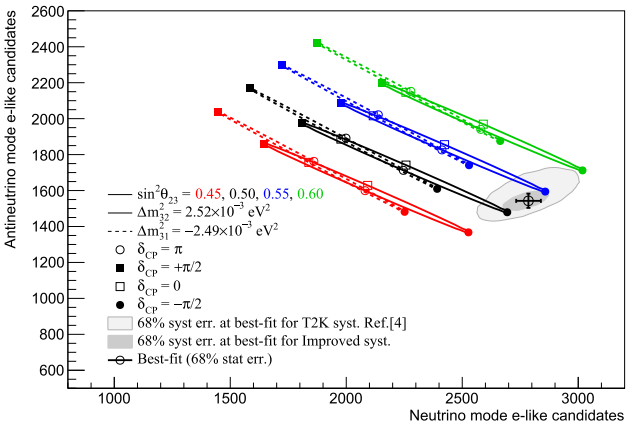

Fig. 3 Fit results with statistical and systematic uncertainties projected on the number of electron (anti)neutrino candidates after 10 years of data taking. The expected number of events for different values of the oscillation parameters is shown for comparison

4 Results

The results of the fit to the oscillation parameters, on a sample corresponding to 10 years of Hyper-Kamiokande data, is projected in Fig. 3 on the number of electron (anti)neutrino candidates, the most relevant samples for the CPV search. The best fit and its statistical and systematic uncertainties are compared to the expected number of events for different values of the oscillation parameters.

The Hyper-Kamiokande sensitivity for CPV discovery as a function of time is shown in Fig. 4. In the case of maximal CPV, $\delta_{CP} = -\pi/2$, Hyper-Kamiokande reaches a definitive 5σ discovery in less than three years. Even with a very conservative assumption on the systematic uncertainties (same values as in T2K in Ref. [4]), Hyper-Kamiokande will reach 5σ sensitivity in less than 6 years. Given the extremely fast discovery scenario for such a case, the possibility of a still partially unknown MO should be considered. If we consider the degenerate case of $\delta_{CP} = -\pi/2$ and inverted ordering and the Hyper-Kamiokande sensitivity to MO using atmospheric and beam data [12], the CPV discovery would be delayed to 6 years also in the case of improved systematic uncertainties. Such estimation is obtained by considering the MO determination with atmospheric Hyper-Kamiokande data as an external constrain to the CPV search with Hyper-Kamiokande beam data. This is a conservative estimate, since it does not consider external measurements of MO from other experiments, nor the boost in CPV sensitivity obtained by a full joint fit of beam and atmospheric data in Hyper-Kamiokande, as performed for instance by the T2K and Super-Kamiokande collaborations in Ref. [44]. Such joint Hyper-Kamiokande beam-atmospheric analysis is being performed for Hyper-Kamiokande and its sensitivity will be reported in a future paper.

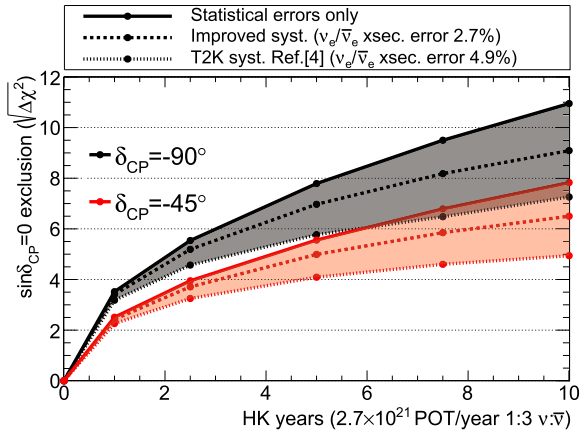

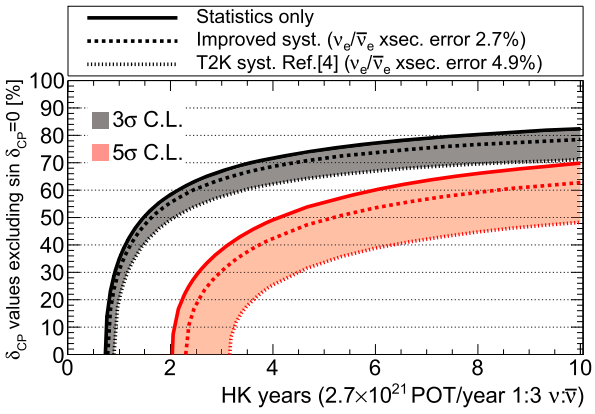

Fig. 4 Sensitivity to CPV as a function of data-taking time: $\sin\delta_{CP} = 0$ exclusion for $\delta_{CP} = -\pi/2$ or $-\pi/4$ (left) and percentage of δ_{CP} values for which $\sin\delta_{CP} = 0$ can be excluded at 3σ and at 5σ (right). The shaded regions in these and following figures, show the span of possible sensitivities when varying the assumed systematic errors

If CP is not maximally violated, assuming known MO, after about six years, Hyper-Kamiokande will be able to discover CPV at 3σ (5σ) for 75% (55%) of possible actual values of δ_{CP}. For instance, a CPV discovery could be achieved in under 6 years in case of $\delta_{CP} = -\pi/4$. The fraction of possible actual values of δ_{CP} for which Hyper-Kamiokande can discover CPV at 3σ (5σ) with 10-years exposure is about 80% (60%). These fractions of δ_{CP} values increase (decrease) by few percent by changing the value of $\sin^2\theta_{23}$ to 0.4 (0.6) and they are independent on the actual MO. The systematic error which most degrades the sensitivity of Hyper-Kamiokande to CPV is the uncertainty on the $\sigma(\nu_e)/\sigma(\bar{\nu}_e)$ cross-section ratio.

The expected resolution of the δ_{CP} measurement is shown in Fig. 5. The achievable resolution depends on the actual value of δ_{CP}, where better resolution can be achieved for values of δ_{CP} close to those where CP is conserved. The most relevant systematic uncertainties are also different depending on the actual value of δ_{CP}. In Fig. 5, two scenarios for the improved systematic error model with different constraints on $\sigma(\nu_e)/\sigma(\bar{\nu}_e)$ are tested. To evaluate the resolution achievable for the measurement of δ_{CP}, we have to consider the derivative with respect to δ_{CP} of the oscillation formula in Eq. 2:

$$\begin{aligned}\partial P(\nu_\mu \to \nu_e)/\partial\delta_{CP} &= -8c_{13}^2 c_{12}c_{23}s_{12}s_{13}s_{23}\cos\delta_{CP} \\ &\cdot \sin\Delta_{32}\cdot\sin\Delta_{31}\cdot\sin\Delta_{21} + 8c_{13}^2 s_{12}s_{13}s_{23}c_{12}c_{23} \\ &\times \sin\Delta_{21}\sin\delta_{CP}(s_{12}^2\sin\Delta_{21} - \cos\Delta_{32}\sin\Delta_{31}). \quad (5)\end{aligned}$$

For the case of CP-conservation ($\delta_{CP} = 0, \pi$), the CP-odd term ($\sin\delta_{CP}$) goes to 0 but its derivative ($\cos\delta_{CP}$) is maximal, thus the precision on the δ_{CP} measurement is dominated by this CP-odd term. Therefore, the precision measurement of δ_{CP} around the CP-conserving values is mostly a rate measurement of the difference between ν_e and $\bar{\nu}_e$, thus the $\sigma(\nu_e)/\sigma(\bar{\nu}_e)$ ratio has a significant impact on the resolution, as is the case for the CP-violation discovery sensitivity. This explains why the green line in Fig. 5 indicates worse resolution than the red line, especially for $\delta_{CP} \simeq 0, \pi$. For the case of maximal CP-violation, the situation is opposite: the CP-even term ($\cos\delta_{CP}$) goes to 0 while its derivative ($-\sin\delta_{CP}$) is maximal, thus dominating the resolution on the δ_{CP} measurement. In this case, the precision is not dominated by the rate asymmetry in the (anti)neutrino electron appearance channels, but by $\cos\delta_{CP}$-induced shape effects on their energy spectra. Thus, for these values of $\delta_{CP} \simeq \pm\pi/2$, making a precise measurement of δ_{CP} is more challenging in terms of statistics and requires very good control of systematic effects related to the neutrino reconstructed energy, such as the far detector energy scale. As a consequence, the resolution worsens for $\delta_{CP} \simeq \pm\pi/2$, as visible in Fig. 5. Moreover the $\sigma(\nu_e)/\sigma(\bar{\nu}_e)$ uncertainty does not dominate (the green line is close to the red line for $\delta_{CP} \simeq \pm\pi/2$), and other systematic uncertainties have an important impact on the measurement.

Finally, the δ_{CP} resolution have a small dependence on the value of $\sin^2\theta_{23}$. Considering $\sin^2\theta_{23} = 0.4$, the δ_{CP} resolution improves by about 2 (0.5) degrees for $\delta_{CP} = -\pi/2$ (0). Considering $\sin^2\theta_{23} = 0.6$, the resolution degrades by about 1 degree for all δ_{CP} values.

Beyond the search for CPV, Hyper-Kamiokande will also feature unprecedented precision on the so-called atmospheric neutrino oscillation parameters. The sensitivity to exclude the wrong θ_{23} octant is defined as

$$\sqrt{\chi^2_{min}(\sin^2\theta_{23})_{WO} - \chi^2_{min}(\sin^2\theta_{23})_{RO}} \quad (6)$$

where the labels WO and RO refer, respectively, to the wrong and right octant. This sensitivity is evaluated through

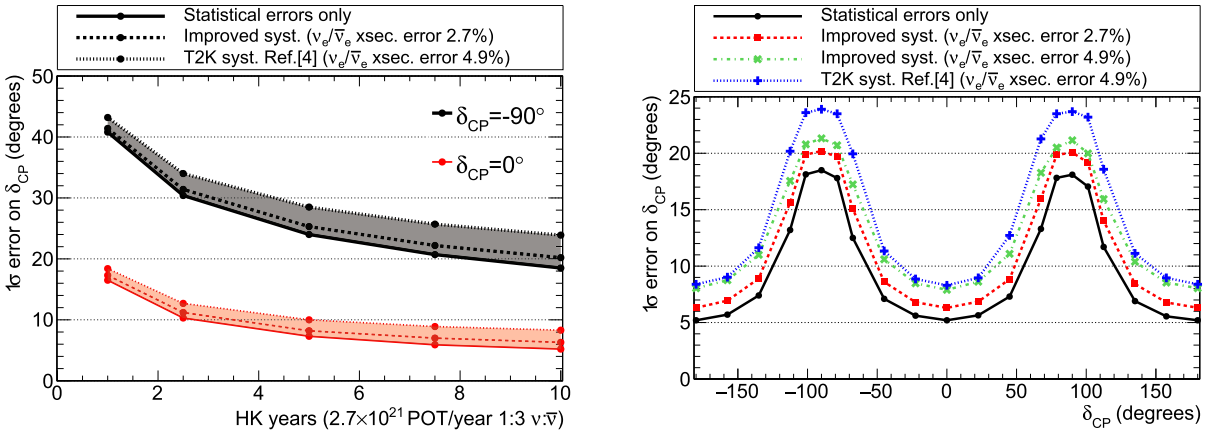

Fig. 5 1σ error on δ_{CP} as a function of data-taking time assuming $\delta_{CP} = -\pi/2$ or 0 (left) and as a function of the value of δ_{CP} after 10 years of data taking (right). Results with different uncertainties on $\sigma(\nu_e)/\sigma(\bar{\nu}_e)$ are shown

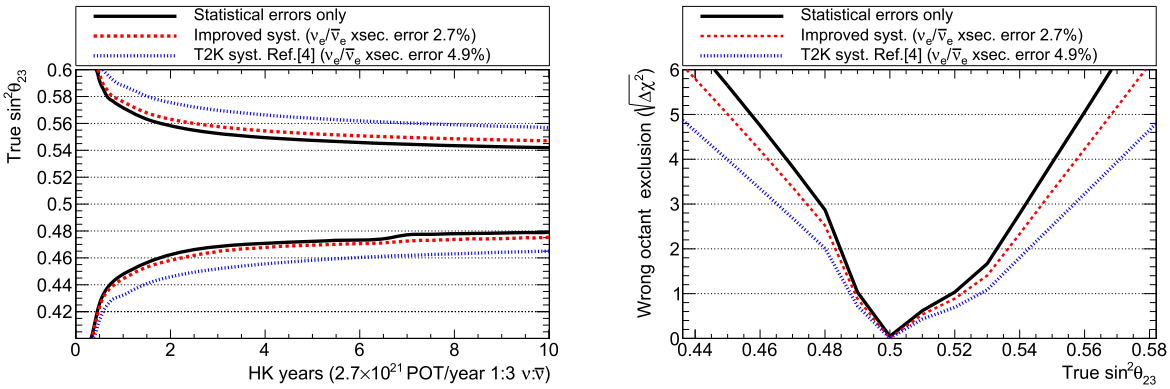

Fig. 6 θ_{23} region, as a function of data-taking time, for which 3σ exclusion of the wrong θ_{23} octant can be reached (left). Sensitivity to the wrong θ_{23} octant exclusion as a function of θ_{23} value after 10 years of data taking (right)

Table 4 Regions of values of $\sin^2\theta_{23}$ for which an exclusion of the wrong octant at 3σ or 5σ is possible after 10 years of data taking

	C.L. 3σ	C.L. 5σ
Stat. only	$[0, 0.48] \cup [0.54, 1]$	$[0, 0.46] \cup [0.56, 1]$
Improved syst	$[0, 0.47] \cup [0.55, 1]$	$[0, 0.45] \cup [0.57, 1]$
T2K syst. in [4]	$[0, 0.46] \cup [0.56, 1]$	$[0, 0.43] \cup [0.59, 1]$

the likelihood scan of a single fit for each true value of θ_{23}. The Hyper-Kamiokande sensitivity to exclude the wrong θ_{23} octant, as a function of the true value of θ_{23}, is shown in Fig. 6 and summarized in Table 4.

Figure 7 shows the resolution on the $\sin^2\theta_{23}$ mixing parameter achievable by Hyper-Kamiokande. Depending on the actual value of the parameter, an ultimate resolution between 2% and 0.4% can be reached. The most challenging region is the case of maximal mixing, where the derivative of the oscillation probability is small and the resolution is directly affected by the octant degeneracy.

The ultimate resolution achievable by Hyper-Kamiokande on Δm^2_{32} is around 0.4%, as shown in Fig. 8. This resolution does not depend sizeably on the actual value of the oscillation parameters. Reaching such precision will require an extremely robust model of systematic uncertainties, notably considering the detector energy scale calibration and the constraint on the nuclear removal energy. In turn, such extremely precise measurement of Δm^2_{32} has important consequences in joint fits with reactor measurements for the determination of the MO [45,46].

Finally, the ultimate Hyper-Kamiokande precision on the $\sin^2\theta_{13}$ parameter is not competitive with measurements from reactor experiments, as shown in Fig. 9. The $\sin^2\theta_{13}$ measurement at long baseline experiments has a degeneracy with the $\sin^2\theta_{23}$ parameter, with the two θ_{23} octants corresponding to the two lobes of the likelihood shown in Fig. 9. Such degeneracy is also visible in the 2D contours shown in Fig. 10 (top). The reactor constraints solve this degeneracy, thus Hyper-Kamiokande data will enable a relative improvement on $\sin^2\theta_{13}$ precision of about 14–23% depending on the systematic uncertainties. The 2D contours

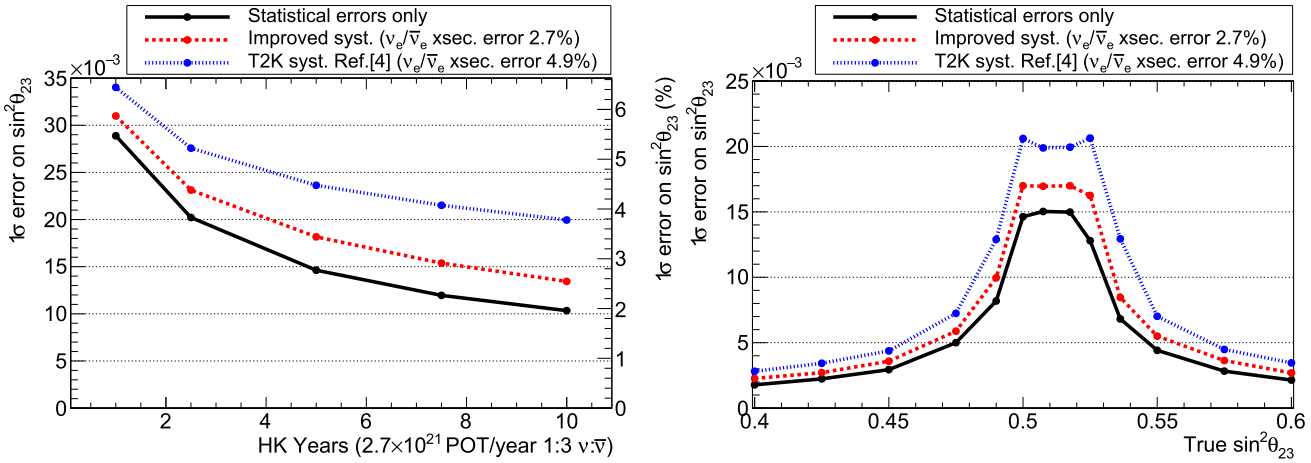

Fig. 7 1σ error on $\sin^2\theta_{23}$ as a function of data-taking time for $\sin^2\theta_{23} = 0.528$ (left) and as a function of $\sin^2\theta_{23}$ value after 10 years of data taking (right)

in δ_{CP} versus $\sin^2\theta_{13}$ are shown in Fig. 10 (bottom), where it can be seen that the ultimate Hyper-Kamiokande sensitivity to δ_{CP} is roughly the same with and without an external constraint from reactor measurements. Hyper-Kamiokande, indeed, will collect enough statistics in both neutrino and antineutrino modes to probe the possible existence of CP violation independently from the reactor θ_{13} measurements.

Table 5 summarizes the expected ultimate precision of the oscillation parameter measurements achievable by the Hyper-Kamiokande experiment.

5 Conclusion

This paper describes the analysis to estimate the sensitivity of the Hyper-Kamiokande experiment to long-baseline neutrino oscillation parameters using accelerator (anti)neutrinos. Results are presented for the CPV discovery sensitivity and precision measurements of the oscillation parameters δ_{CP}, $\sin^2\theta_{23}$, Δm^2_{32} and $\sin^2\theta_{13}$. This work is based on the T2K analysis in Ref. [4], with tuning applied to the neutrino flux prediction and the far detector simulation to match the Hyper-Kamiokande design [12]. Different assumptions for the systematic uncertainties are compared, starting with the T2K uncertainties from Ref. [4] and applying further reductions based on the Hyper-Kamiokande expected statistics and the upgraded ND280 and IWCD capabilities.

With the assumed Hyper-Kamiokande running plan, a 5σ CPV discovery is possible in less than three years in the case of maximal CPV and known MO. In the absence of external constraints on the MO, considering the MO sensitivity of the Hyper-Kamiokande measurement using atmospheric neutrinos, the time for a CPV discovery could be estimated to be around 6 years. We defer a detailed joint Hyper-Kamiokande beam-atmospheric neutrino analysis to a future publication.

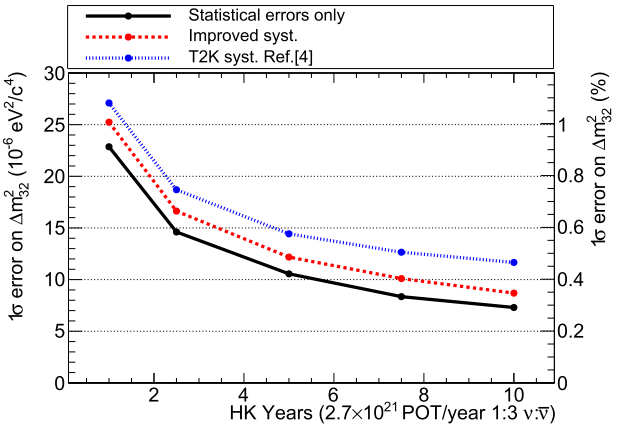

Fig. 8 1σ error on Δm^2_{32} as a function of data-taking time

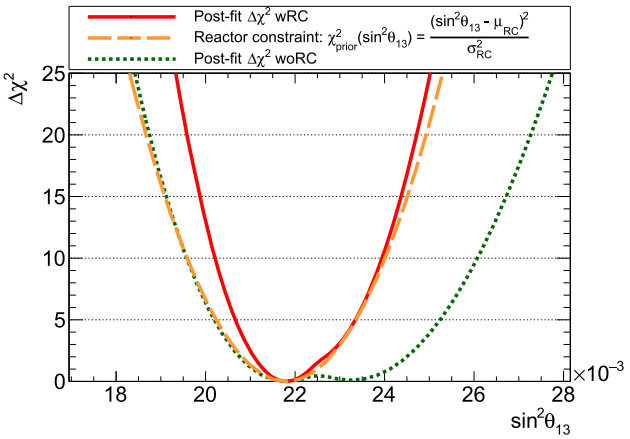

Fig. 9 Measurement of θ_{13}: $\Delta\chi^2(\sin^2\theta_{13})$ curves in the "Improved syst." error model, after 10 years of data-taking, with (wRC) and without (woRC) the external constraint from reactor measurements

Table 5 Summary of the 1σ expected resolution of the oscillation parameters after 10 years of data taking. The numbers in percentage are relative errors

Parameter and true value	$\delta_{CP} = 0$	$\delta_{CP} = -\pi/2$	$\sin^2\theta_{23} = 0.528$	$\Delta m^2_{32} = 2.509 \times 10^{-3}$ eV^2/c^4	$\sin^2\theta_{13} = 0.0218$ (with RC)
Statistics only	5.2°	18.5°	0.0103	7.30×10^{-6}	4.73×10^{-4}
			1.95%	0.29%	2.17%
Improv. systematics	6.3°	20.2°	0.0134	8.69×10^{-6}	5.39×10^{-4}
			2.54%	0.35%	2.47%
T2K systematics in [4]	8.3°	23.9°	0.0199	11.62×10^{-6}	6.04×10^{-4}
			3.77%	0.46%	2.77%

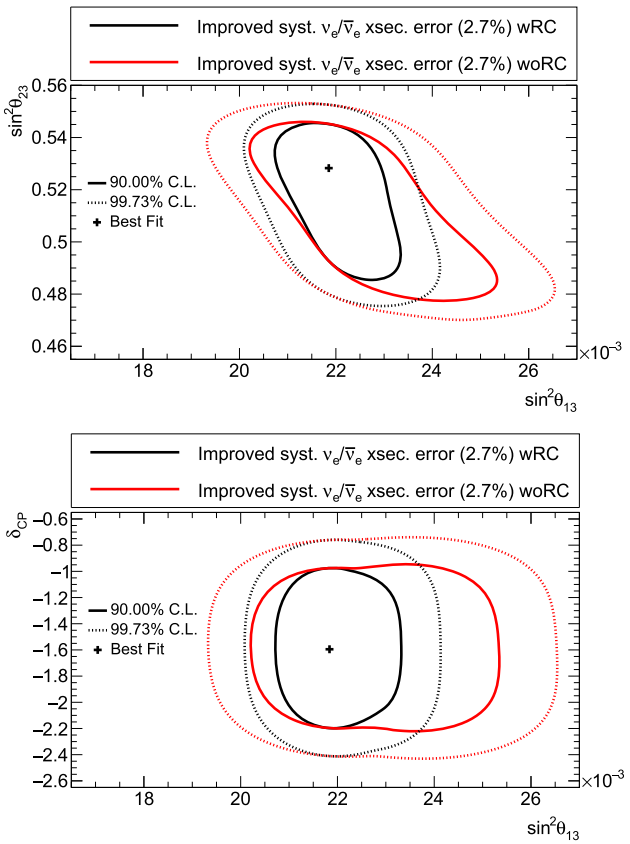

Fig. 10 Confidence level contours: $\sin^2\theta_{23}$ vs. $\sin^2\theta_{13}$ (top) and δ_{CP} vs. $\sin^2\theta_{13}$ (bottom) after 10 years of data-taking, with the "Improved syst." error model, with (wRC) and without (woRC) external constraint from reactor θ_{13} measurements

Using the nominal final exposure of 27×10^{21} protons on target, corresponding to 10 years, with a ratio of 1:3 in neutrino to antineutrino beam mode, we expect to select approximately 10,000 charged current, quasi-elastic-like, muon neutrino events, and a similar number of muon antineutrino events. In the electron (anti)neutrino appearance channels, we expect approximately 2000 charged current, quasi-elastic-like electron neutrino events and 800 electron antineutrino events, assuming $\delta_{CP} = -1.601$. These large event samples will allow Hyper-Kamiokande to exclude CP conservation at the 5σ significance level for over 60% of the possible true values of δ_{CP}. Depending on the value of δ_{CP}, Hyper-Kamiokande can measure the δ_{CP} parameter to a precision of about 6° (in the case of CP conservation) or 20° (in the case of maximal CPV). The wrong $\sin^2\theta_{23}$ octant can be excluded at a significance above 5σ for $\sin^2\theta_{23} < 0.45$ and $\sin^2\theta_{23} > 0.57$. The value of $\sin^2\theta_{23}$ can be measured with a precision of around 3% in the most challenging region of maximal disappearance and better than 0.5% otherwise. The expected precision on the measurement of Δm^2_{32} is better than 0.5%.

With the assumed running ratio of 1:3 for neutrino to antineutrino beam mode operation, the Hyper-Kamiokande ultimate δ_{CP} resolution is mainly independent of the constraint on $\sin^2\theta_{13}$ from external reactor measurements. Still, this reactor constraint reduces the degeneracy between $\sin^2\theta_{13}$ and $\sin^2\theta_{23}$. When the reactor constraint on $\sin^2\theta_{13}$ is applied and thus the degeneracy resolved, Hyper-Kamiokande will be able to slightly improve the precision on the measurement of $\sin^2\theta_{13}$ with respect to the reactor measurement.

Acknowledgements The Hyper-Kamiokande Collaboration would like to thank the Japanese Ministry of Education, Culture, Sports, Science and Technology (MEXT), the University of Tokyo, Japan Society for the Promotion of Science (JSPS), the Kamioka Mining and Smelting Company, Japan; the Minister of Education, Science, Culture and Sports, grant 21T-1C333, Armenia; CNPq and CAPES, Brazil; Ministry of Education Youth and Sports of the Czech Republic (FORTE CZ.02.01.01/00/22_008/0004632); CEA and CNRS/IN2P3, France; the INFN, Italy; the National Science Foundation, the Korea National Research Foundation (No. NRF 2022R1A3B1078756), Korea; CONAHCyT for supporting the national projects CBF2023-2024-427, and CF-2023-G-643., Mexico; Ministry of Science and Higher Education (2022/WK/15) and the National Science Centre (UMO-2022/46/E/ST2/00336), Poland; MICIU, Spain and NextGenerationEU/PRTR, EU, Spain; ETHZ, SERI and SNSF, Switzerland; STFC and UKRI, UK. We also thank CERN for use of the Neutrino Platform. In addition, the participation of individual researchers and institutions has been further supported by funds from Charles University (Grant PRIMUS 23/SCI/025 and Research Center UNCE/24/SCI/016), Czech Republic; H2020-MSCA-RISE-2019 SK2HK no 872549 and H2020 Grant No. RISE-GA822070-JENNIFER2 2020, Europe; JSPS KAKENHI Grant JP24K17065; National Research Foundation of Korea (NRF-2022R1A5A1030700, NRF-2022R1A3B1078756) funded by

the Ministry of Science, Information and Communication Technology (ICT) and the Ministry of Education (RS-2024-00442775), Korea; Associate Dean of Research and Scientific Graduate Studies, Dr. Daniel A. Jacobo-Velázquez, for his support and also to CONAHCyT for the postgraduate scholarship 835328; Rector of the CUCEI, Dr. Marcos Pérez, for his financial and logistical support and CONAHCyT for the information technologies doctoral scholarship 792151, Mexico; Ministry of Science and Higher Education, Republic of Poland, "International co-financed projects", grant number 5316/H2020/2022/2023/2, Poland; LSC funds from MICIU, DGA and UZ, Spanish Ministry of Science and Innovation PID2022-136297NB-I00 /AEI/10.13039/501100011033/ FEDER, UE; CERCA program of the Generalitat de Catalunya; Plan de Doctorados Industriales of the Research and Universities Department of the Catalan Government (2022 DI 011); MICIIN; European Union NextGenerationEU(PRTR-C17.I1); generalitad de Catalunya; Spanish Ministry of Innovation and Science under grants MCINN-23-PID2022-139198NB-I00 and PID2021-124050NB-C31, Spain; SNF 20FL20-216674, SNF 200021 L-231581 and SNF PCEFP2-203261, Switzerland; the Leverhulme Trust Research Fellowship Scheme and the UKRI Future Leaders Fellowship grant number MR/S034102/1, UK. The Hyper-Kamiokande Collaboration would like to thank the T2K Collaboration for providing the models and simulated samples used as a basis in this paper.

Data Availability Statement This manuscript has no associated data. [Authors' comment: Data sharing not applicable to this article as no datasets were generated or analysed during the current study.]

Code Availability Statement This manuscript has no associated code/software. [Authors' comment: Code/Software sharing not applicable to this article as no code/software was generated or analysed during the current study.]

Funded by SCOAP[3].

References

1. B. Pontecorvo, Z. Eksp, Teor. Fiz. **53**, 1717 (1967)
2. Z. Maki, M. Nakagawa, S. Sakata, Prog. Theor. Phys. **28**, 870 (1962). https://doi.org/10.1143/PTP.28.870
3. S. Navas et al., Phys. Rev. D **110**(3), 030001 (2024). https://doi.org/10.1103/PhysRevD.110.030001
4. K. Abe et al., Eur. Phys. J. C **83**(9), 782 (2023). https://doi.org/10.1140/epjc/s10052-023-11819-x
5. M.A. Acero et al., Phys. Rev. D **110**(1), 012005 (2024). https://doi.org/10.1103/PhysRevD.110.012005
6. M. Fukugita, T. Yanagida, Phys. Lett. B **174**, 45 (1986). https://doi.org/10.1016/0370-2693(86)91126-3
7. A. Granelli, S. Pascoli, S.T. Petcov, Phys. Rev. D **108**(10), L101302 (2023). https://doi.org/10.1103/PhysRevD.108.L101302
8. T. Wester et al., Phys. Rev. D **109**(7), 072014 (2024). https://doi.org/10.1103/PhysRevD.109.072014
9. A. Abud Abed et al., Phys. Rev. D 105(7), 072006 (2022). doi: 10.1103/PhysRevD.105.072006
10. J. Gehrlein, S. Petcov, M. Spinrath, A. Titov (2022). arXiv:2203.06219
11. K. Abe et al., PTEP 2015, 053C02 (2015). doi: 10.1093/ptep/ptv061
12. K. Abe et al. (2018). arXiv:1805.04163
13. K. Hirata et al., Phys. Rev. Lett. **58**, 1490 (1987). https://doi.org/10.1103/PhysRevLett.58.1490
14. Y. Fukuda et al., Nucl. Instrum. Methods A **501**, 418 (2003). https://doi.org/10.1016/S0168-9002(03)00425-X
15. M.H. Ahn et al., Phys. Rev. D **74**, 072003 (2006). https://doi.org/10.1103/PhysRevD.74.072003
16. K. Abe et al., Nucl. Instrum. Methods A **659**, 106 (2011). https://doi.org/10.1016/j.nima.2011.06.067
17. K. Abe et al. (2019). arXiv:1908.05141
18. K. Abe et al., Nucl. Instrum. Methods A **694**, 211 (2012). https://doi.org/10.1016/j.nima.2012.03.023
19. K. Abe et al. (2019). arXiv:1901.03750
20. S. Bhadra et al. (2014). arXiv:1412.3086
21. C.A. Argüelles et al., Eur. Phys. J. C **83**(1), 15 (2023). https://doi.org/10.1140/epjc/s10052-022-11049-7
22. R. Davis Jr., D.S. Harmer, K.C. Hoffman, Phys. Rev. Lett. **20**, 1205 (1968). https://doi.org/10.1103/PhysRevLett.20.1205
23. M. Altmann et al., Phys. Lett. B **616**, 174 (2005). https://doi.org/10.1016/j.physletb.2005.04.068
24. J.N. Abdurashitov et al., Phys. Rev. C **80**, 015807 (2009). https://doi.org/10.1103/PhysRevC.80.015807
25. G. Bellini et al., Phys. Rev. Lett. **107**, 141302 (2011). https://doi.org/10.1103/PhysRevLett.107.141302
26. B. Aharmim et al., Phys. Rev. C **88**, 025501 (2013). https://doi.org/10.1103/PhysRevC.88.025501
27. K. Abe et al., Phys. Rev. D **94**(5), 052010 (2016). https://doi.org/10.1103/PhysRevD.94.052010
28. A. Gando et al., Phys. Rev. D **88**(3), 033001 (2013). https://doi.org/10.1103/PhysRevD.88.033001
29. D. Adey et al., Phys. Rev. Lett. **121**(24), 241805 (2018). https://doi.org/10.1103/PhysRevLett.121.241805
30. C.D. Shin et al., JHEP **04**, 029 (2020). https://doi.org/10.1007/JHEP04(2020)029
31. H. de Kerret et al., Nat. Phys. **16**(5), 558 (2020). https://doi.org/10.1038/s41567-020-0831-y
32. V.D. Barger, K. Whisnant, S. Pakvasa, R.J.N. Phillips, Phys. Rev. D **22**, 2718 (1980). https://doi.org/10.1103/PhysRevD.22.2718
33. R. Wendell, Prob3++ (2018). https://github.com/rogerwendell/Prob3plusplus. Consulted on 2024
34. A. Abusleme et al. (2024). arXiv:2405.18008
35. S. Aiello et al., Eur. Phys. J. C **82**(1), 26 (2022). https://doi.org/10.1140/epjc/s10052-021-09893-0
36. P. Eller et al., PoS ICRC2023, 1036 (2023). https://doi.org/10.22323/1.444.1036
37. K. Abe et al., Phys. Rev. D **87**(1), 012001 (2013). https://doi.org/10.1103/PhysRevD.87.012001. [Addendum: Phys. Rev. D 87, 019902 (2013)]
38. N. Abgrall et al., Eur. Phys. J. C **76**(11), 617 (2016). https://doi.org/10.1140/epjc/s10052-016-4440-y
39. K. Abe et al., Phys. Rev. D **103**(11), 112008 (2021). https://doi.org/10.1103/PhysRevD.103.112008
40. S. Dolan et al., Phys. Rev. D **105**(3), 032010 (2022). https://doi.org/10.1103/PhysRevD.105.032010
41. L. Munteanu, S. Suvorov, S. Dolan, D. Sgalaberna, S. Bolognesi, S. Manly, G. Yang, C. Giganti, K. Iwamoto, C. Jesús-Valls, Phys. Rev. D **101**(9), 092003 (2020). https://doi.org/10.1103/PhysRevD.101.092003

42. T. Dieminger, S. Dolan, D. Sgalaberna, A. Nikolakopoulos, T. Dealtry, S. Bolognesi, L. Pickering, A. Rubbia, Phys. Rev. D **108**, L031301 (2023). https://doi.org/10.1103/PhysRevD.108.L031301
43. O. Tomalak, Q. Chen, R.J. Hill, K.S. McFarland, Nat. Commun. **13**(1), 5286 (2022). https://doi.org/10.1038/s41467-022-32974-x
44. K. Abe et al. (2024). arXiv:2405.12488
45. H. Nunokawa, S.J. Parke, R. Zukanovich Funchal, Phys. Rev. D 72, 013009 (2005). https://doi.org/10.1103/PhysRevD.72.013009
46. S.J. Parke, R. Zukanovich-Funchal (2024). arXiv:2404.08733